Universitat Autònoma de Barcelona

EVALUACIÓN DE LOS CAMBIOS EN EL MIOCARDIO DE ADOLESCENTES CON OBESIDAD MÓRBIDA. EVALUATION OF MYOCARDIAL CHANGES IN ADOLESCENTS WITH MORBID OBESITY

José Manuel Siurana Rodríguez

TESIS DOCTORAL

EVALUACIÓN DE LOS CAMBIOS EN EL MIOCARDIO DE ADOLESCENTES CON OBESIDAD MÓRBIDA.

EVALUATION OF MYOCARDIAL CHANGES IN ADOLESCENTS WITH MORBID OBESITY

José Manuel Siurana Rodríguez

Directoras de Tesis:

Dra. Anna Sabaté Rotés

Dra. Paula Sol Ventura Wichner

Tutor de Tesis:

Dr. Antonio Moreno

Programa de Doctorat en Pediatria, Obstetrícia i Ginecologia

Departament de Pediatria, d'Obstetrícia i Ginecologia, i Medicina Preventiva i Salut Pública

Universitat Autònoma de Barcelona

2022

Para Ana, Clara y Julia

AGRADECIMIENTOS

Mis tutoras, Paula Sol Ventura y Anna Sabaté, cuyos conocimientos y trabajo están plasmados en esta tesis doctoral. Les agradezco enormemente su confianza y todas las horas que me han regalado.

Mis compañeros del Hospital de Nens, empezando por Álvaro Díaz, Lluís Cabero y Javier Massaguer, cuyo estímulo y apoyo me hizo embarcarme en este proyecto, y los miembros del servicio de cardiología, a los cuales quiero agradecer su ayuda diaria y su paciencia conmigo: Regina, Georges, Yanira, Sergio, Isabel, Manuela, Mónica, Susana, Juani, Noelia, Julisa y Anna. También a todos los pediatras y endocrinólogos de las consultas externas que colaboraron en la reclutación de pacientes.

Esta tesis doctoral no hubiera sido la que es sin la inestimable y desinteresada ayuda de los servicios de endocrinología, cardiología y radiología del Hospital Materno Infantil Vall d'Hebron. El Dr. Diego Yeste merece mi más sincero agradecimiento por su liderazgo y apoyo para que este proyecto saliera adelante. Agradecer también a la Dra. Riaza el tiempo y conocimientos dedicados, pues su trabajo ha constituido una pieza clave.

El laboratorio de metabolómica Biosfer Teslab y todo su equipo liderado por la Dra. Amigó, que junto con la Dra. Martínez-Micaelo, me iniciaron en el conocimiento molecular de las lipoproteínas y las vías metabólicas implicadas en la fisiopatología de la obesidad. Gracias por el tiempo y la paciencia que dedicaron en mi formación. Igualmente quiero agradecer la colaboración del laboratorio Durán i Bellido, en especial a las compañeras de extracción de sangre, y del laboratorio del Hospital Vall d'Hebron.

La Sociedad Española de Cardiología Pediátrica colaboró económicamente para que este proyecto fuera una realidad al concederle la beca Juan V Comas del año 2019 y el premio a la mejor comunicación en el 13ª congreso nacional del año 2020.

Mis amigos de universidad han sido una constante fuente de estimulación intelectual, estímulo y apoyo. Empezando por mis apreciadas amigas Elisabet y Cristina, además de Raül, Quim, Natalia, Judit, Nano, Celia, Cristina, Edu, Eva, Pablo, Laura y Marta.

Mis padres, Manolo y Amparo, me mostraron con su ejemplo el camino de la perseverancia y la constancia. Mi hermano Víctor con el que comparto vida y del que tantas cosas buenas aprendo cada año, y mi hermano Javi, fallecido a los 8 años, del que guardo el mejor recuerdo y cuyo espíritu marca mi sino en la vida. Mis hijas, Clara y Julia, son el faro que ilumina mi vida y el motor de amor y responsabilidad que me impulsa hacia adelante cada día.

Y finalmente, mi más profunda deuda de gratitud, por su optimismo, apoyo e inagotable confianza, es para mi querida esposa, Ana.

CONTENTS

ABBREVIATIONS

ALT, Advanced Lipid Test

BMI, Body Mass Index

BP, Blood Pressure

CLP, Conventional Lipid Profile

CMR, Cardiovascular Magnetic Resonance

CVD, Cardiovascular Disease

DBP, Diastolic Blood Pressure

ECM, Extracellular Matrix

GLS; Global Longitudinal Strain

GLSR, Global Longitudinal Strain Rate

GlycA, Glycoprotein A

HDL, High-density Lipoprotein

HDL-C, Cholesterol in High-density Lipoprotein

HDL-P, Particles of High-density Lipoprotein

HFF, Hepatic Fat Fraction

HOMA-IR, Homeostasis model assessment of insulin resistance

hs-CRP, Highly sensitive C-reactive Protein

IDL, Intermediate-density Lipoprotein

LDL, Low-density Lipoprotein

LDL-C, Cholesterol in Low-density Lipoprotein

LDL-P, Particles of Low-density Lipoprotein

LV, Left Ventricle

MHO, Metabolically Healthy Obesity

MS, Metabolic Syndrome

MUO, Metabolically Unhealthy Obesity

PFI, Pericardial Fat Index

RWT, Relative Wall Thickness

SBP, Systolic Blood Pressure

TG, Triglycerides

TMI, Triponderal Mass Index

T2-DM, Type 2 Diabetes Mellitus

VLDL, Very low-density Lipoprotein

VLDL-P, Particles of Very low-density Lipoprotein

1H-NMR, Positron Nuclear Magnetic Resonance Spectrometry

2DSTE, Two-dimensional Speckle Tracking Echocardiography

1. INTRODUCTION

1.1 Pandemic Obesity

The fact that the world has an obesity pandemic becoming worse in recent decades is widely known up to the point that the World Health Organization included the reduction of obesity as one of the main targets of the Global Action Plan for the Prevention and Control of Noncommunicable Diseases 2013–2020.[1] Pediatric obesity is the starting point for future health problems[2] – cardiovascular disease (CVD), type 2 diabetes mellitus, cerebrovascular disease, heart failure –, so the identification of subjects at significant risk is an urgent task to avoid future irreversible changes. Spain is one of the countries with the highest percentage of children with obesity in Europe (7-13 years old: 32%), and the children's overweight percentage has increased by 38% since 1990, becoming the fastest growth rate amongst OECD countries.[3] The percentage of severe obesity in childhood is not well known in Spain, because of the lack of consensus on its definition: Body Mass Index (BMI) +3.5 SD, BMI ≥35 kg/m^2 or BMI percentage respect to the 95th percentile of 120-140% for severe obesity and >140% for morbid obesity.

1.2 Obese Phenotypes

Some prospective studies have described a group of individuals with obesity as having metabolically healthy obesity (MHO), due to the lack of overt cardiometabolic abnormalities.[4] Despite the different proposed defining criteria for this condition,[5-7] the MHO prevalence in adults has been estimated at 12% in European countries[6] and 20-35% in children.[2] The prevalence among children and adolescents in Catalonia, where our study was conducted, is 37%.[8] MHO patients are younger and with a peripheral fat distribution, while subjects with metabolically unhealthy obesity (MUO) present increased intra-abdominal fat mass, liver fat content and infiltrative fat in skeletal muscle, which predispose to insulin-resistance and cardiometabolic events. Nevertheless, while MHO is associated with less risk, these subjects should not be identified as healthy patients because transition to MUO over time occurs frequently.[4,9] Unfortunately, there are few studies conducted in children with morbid obesity and the evaluation of myocardial index in MHO compared to MUO patients has been hardly evaluated.[10]

1.3 Cardiovascular Risk Factors in Obesity

Cardiovascular diseases are the main cause of death in the world[11] and, if the trend initiated in 2000 continues, CVD will also become the main cause of death among contemporary children. Obesity is a multifactorial disease that includes several preceding disorders of CVD, such as high blood pressure (BP), insulin resistance, diabetes and dyslipidemia. However, the majority of obese children present a pre-pathological condition.

In the conventional lipid profile (CLP), the increase in cholesterol in low-density lipoproteins (LDL-C) has been demonstrated as one of the most important factors associated with CVD risk,[12] but the role of high-density lipoprotein cholesterol (HDL-C) or triglycerides (TG) remains unclear.[13] Additionally, the remnant cholesterol – a derivative from the CLP that accounts for the cholesterol enclosed in the very low-density lipoproteins (VLDL), intermediate-density lipoproteins (IDL) and chylomicrons – has been also associated with increased prevalence of ischemic heart disease[14] and myocardial infarction.[15] On the other hand, the advanced lipoprotein testing (ALT), assessed by proton nuclear magnetic resonance spectroscopy (1H-NMR) of plasma, provides much information about lipoprotein characteristics as it quantifies the concentration, particle size and composition (cholesterol or TG) of each lipoprotein subclass. Previous studies have shown how in situations of apparent normality, specific lipoprotein alterations are highly associated with future CVD events.[16-19] Thus, the concept of atherogenic dyslipidemia – applied to subjects with hypo HDL-C, hypertriglyceridemia and normal LDL-C, but increases in some ALT components – has been associated with an elevated risk of CVD events.[20-22]

Various studies have evaluated the ALT in obese adults and adolescents and established its utility in predicting arterial wall changes, coronary heart disease or CVD events,[23-25] however to our knowledge, none have analyzed which ALT components are closely associated with cardiac changes in obese adolescents.

1.4 Left Ventricular Changes in Obesity

It has been demonstrated that obesity increases the risk of heart failure and CVD in adulthood,[26] and that adolescents with severe obesity present elevated risk for future CVD.[27] Major changes noted in the myocardium of subjects with obesity during childhood include: increased left ventricle (LV) myocardial mass and wall thickness, impaired longitudinal and circumferential strain and decreased E/A ratio. Pathological LV geometry has been also well defined in children with obesity, especially in cohorts with high BMI ranges, and in adults it has been associated with early mortality.[28,29] Two-dimensional speckle tracking echocardiography (2DSTE) is a well validated and reproducible method to quantify ventricular function. Strain and strain rate (SR) evaluate myocardial deformation and provide global and regional cardiac function measurements. Compared with LV ejection fraction, global longitudinal strain (GLS) has a superior prognostic value for predicting mortality in adults and exhibits a lower variability in children.[30,31]

Myocardial changes because of obesity are well documented in adults. However, most research in children has been conducted in patients who are overweight or have mild obesity and there are few studies in pediatric populations with morbid obesity, where adverse cardiometabolic risk factors and myocardial dysfunction are more expectable.[32,33] Furthermore, the evaluation of myocardial index in MHO population compared to MUO has generated dissimilar conclusions.[10,34]

1.5 Myocardial Tissue Characterization

Obesity and some of its comorbidities such as hypertension or diabetes mellitus (DM) are pathologies with a high risk of developing secondary non-ischemic cardiomyopathies because of their capacity for triggering changes in the myocardium interstitium – characterized by fibroblast activation, myofibroblast development, inflammation and disrupted formation of metalloproteinases – and leading to modifications of the extracellular matrix (ECM) as well as intrinsic myocardium deteriorations.[35] The non-ischemic cardiomyopathy final stage is characterized by a diffuse myocardial fibrosis, which, unlike with post-infarction cardiomyopathy, possesses a prolonged subclinical course before the onset of symptoms.[36]

T1 mapping is a cardiovascular magnetic resonance (CMR) technique that quantifies changes to the ECM, disrupted as a result of diffuse reactive fibrosis, myocardial edema, substance deposits or myocardial scars.[37-39] T1 mapping has demonstrated its value in assessing myocardial changes in pathologies that involve interstitial fibrosis.[40,41] Conversely, when cardiovascular risk factors induce myocardial changes but no underlying cardiomyopathy, the native T1 time has been unaffected.[42] Therefore, native T1 has demonstrated its utility in differentiating cardiomyopathies from reactive myocardial changes secondary to cardiovascular risk factors. Moreover, due to its capacity for assessing myocardium inflammation and fibrosis, native T1 could be a useful technique for evaluating the impact of obesity's low-grade inflammation in the myocardium and detecting the obese patients at higher risk of developing a non-ischemic cardiomiopathy.[43,44] However, to our knowledge, the few studies

conducted in obese adults have generated opposite conclusions and the obese pediatric population has not been previously evaluated.[45,46]

1.6 Fat Tissue Infiltration

The adipose tissue around the heart is interconnected with the myocardium and has the ability of affecting it by the release of pro-inflammatory molecules such as cytokines and adipokines. The pericardial fat, defined as the sum of the epicardial fat (adipose tissue enclosed within parietal pericardium) and the paracardial fat (adipose tissue confined between the chest wall and the pericardium), has previously been related in children with cardiovascular risk factors and cardiac changes[47] however, no study has assessed its relationship with T1 mapping.

2. RATIONALE FOR THIS RESEARCH

The World Health Organization estimated in 2018 that 40% of children in Spain were overweight or obese. This percentage is one of the highest in Europe and data are worsening year after year. The number of obese children and adolescents in the world increased more than ten times from 11 million in 1975 to 124 million in 2016. Additionally, obese adolescents are largely unsuccessful in losing weight and around 80% will still be obese in adulthood. It is estimated that in Spain in 2030 the overweight and obesity rates will be 80% in men and 55% in women, creating an additional cost for the healthcare system of 3,000 million euros.

This project evaluates the impact of obesity on the cardiovascular system through the analysis of early myocardial changes using highly sensitive novel techniques – Speckle Tracking echocardiography and native T1 mapping – and the quantification of cardiovascular risk by low-grade inflammation specific markers combined with an advanced lipoprotein test. The objective is to identify which adolescents with obesity are at higher risk of developing myocardial changes in order to undertake the most appropriate preventive interventions so as to avoid future irreversible cardiac damages.

3. HYPOTHESIS AND AIMS

3.1. HYPOTHESIS:

Morbidly obese adolescents present myocardial changes as a consequence of their obesity. These changes trigger modifications in the myocardial tissue and are related to a specific metabolic-inflammatory pattern.

3.2. OVERALL AIM:

To evaluate the left ventricular function, the myocardial tissue and their relationship with metabolic-inflammatory patterns in adolescents with morbid obesity.

3.3. SPECIFIC AIMS:

3.3.1. To assess the left ventricle geometry and function by standard echocardiographic measurements and advanced evaluation methods: Tissue Doppler and Speckle Tracking.

3.3.2. To define the applicability of obesity phenotypes in morbidly obese adolescents to predict left ventricular changes.

3.3.3. To establish the metabolic-inflammatory pattern better related to cardiac changes by determining cardiovascular risk factors, inflammatory markers and the advanced lipoprotein test measured by proton nuclear magnetic resonance spectroscopy.

3.3.4. To characterize the myocardial tissue composition by using T1 mapping cardiovascular magnetic resonance and evaluate its usefulness in differentiating obese subjects at high cardiovascular risk.

3.3.5. To evaluate the fat tissue content in heart and liver by quantifying the pericardial fat volume and the hepatic fat fraction.

4. METHODOLOGY

4.1 Study Population and Flow Diagram

For this research 75 adolescents of both genders between 10 and 17 years old were recruited. Subjects with obesity were selected from endocrinology clinics of participating hospitals and control participants were recruited from healthy volunteers in the cardiology and sports medicine clinics. Two main groups were identified: the study group with morbid obesity (SDS-BMI ≥4; n = 48), and the control subjects (BMI 5^{th}-85^{th} percentile, n = 27) according to tables from the Barcelona Longitudinal Growth Study 1995–2017.[48] The control group adolescents were paired by age, gender and Tanner stage, with ratio 2 cases: 1 control, for minimizing the confounding effects.

Five subjects were excluded due to incomplete basic laboratory or image parameters. The flow diagram in Figure 1 shows how many subjects got involved in the different projects carried out to achieve the objectives of this Thesis.

Figure 1: Flow diagram of subjects who got involved in the study

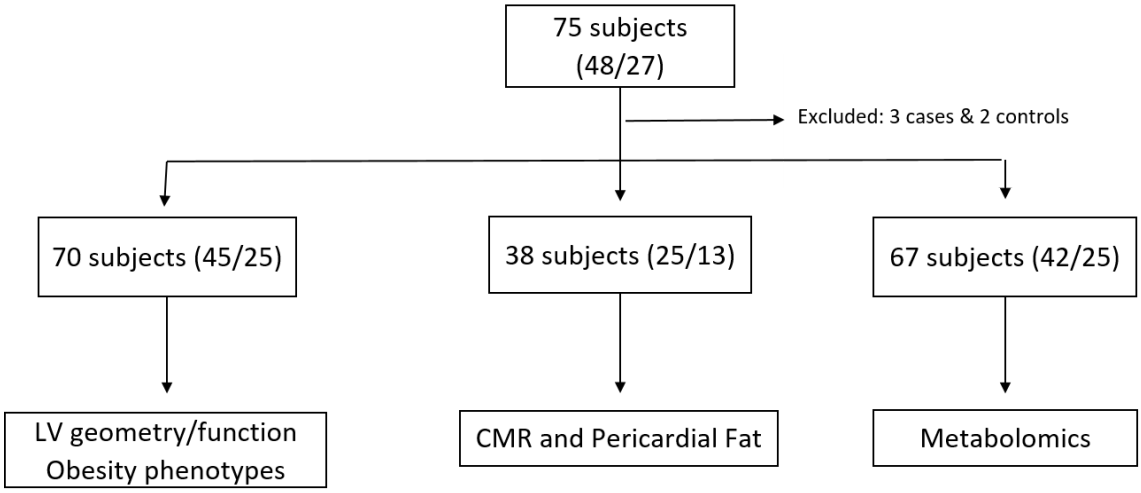

4.2 Inclusion and Exclusion Criteria

Subjects with current infectious or recent acute inflammatory processes, history of prematurity or birth weight <2000 g, and smokers or those with pathologies that could change the arterial or myocardial wall – such as congenital heart disease, chronic kidney disease, transplant, rheumatic diseases, infection by HIV virus – were excluded.

Considering that some subjects were recruited in the sports clinic, weekly sport hours were recorded. This potential confounding variable is poorly detailed in previous studies involving adolescents, although the duration and intensity of regular sports training can cause adaptive LV structural remodeling. An appropriate threshold of weekly sport hours was established according to some studies that defined a regular

athlete when sport practice is more than 9 hours per week.[49] Hence, subjects that practiced >7 hours per week were excluded in this study.

Written informed consent for participation was obtained and the Institutional Review Board at Vall d'Hebron Hospital approved the protocol (PR-AMI-273/2018). All subjects provided assent and informed consent had been signed by their parents/legal guardians.

4.3 Studies Included

This Thesis includes data from three studies involving the same target population but with different evaluations to achieve the overall and specific aims.

I. Left ventricular geometry and function Study and obese phenotype comparative Substudy: Defines the LV geometry and function and its relationship with cardiovascular risk factors, and compares the cardiac impairtment's degree between both obese phenotypes.

II. Lipoprotein particle profiles and cardiac involvement Study: By way of lipoprotein particle and inflammatory marker determinations defines what is the metabolic-inflammatory pattern better related to cardiac changes, BMI and metabolic syndrome.

III. Myocardial tissue characterization and pericardial fat Study: Evaluates the native T1 mapping, the pericardial fat volume and the hepatic fat fraction, and their relationship with cardiovascular risk factors and inflammatory parameters.

5. LEFT VENTRICULAR GEOMETRY AND FUNCTION STUDY

This study has been published at:

Siurana JM, Ventura PS, Yeste D, Riaza-Martin L, Arciniegas L, Clemente M, Torres M, Amigó N, Giralt G, Roses-Noguer F, Sabaté-Rotés A. Myocardial Geometry and Dysfunction in Morbidly Obese Adolescents (BMI 35-40 kg/m^2). Am J Cardiol. 2021;157:128-134. doi: 10.1016/j.amjcard.2021.07.026.

Myocardial Geometry and Dysfunction in Morbidly Obese Adolescents (BMI 35−40 kg/m^2)

Jose M. Siurana, MD[a,b,*], Paula S. Ventura, PhD[a,b], Diego Yeste, PhD[b,c,d], Lucia Riaza-Martin, MD[c], Larry Arciniegas, MD[c], Maria Clemente, PhD[b,c,d], Marisa Torres, MD[a], Núria Amigó, PhD[e], Gemma Giralt, MD[b,c], Ferran Roses-Noguer, PhD[b,c], and Anna Sabate-Rotes, PhD[b,c]

This study evaluated the preclinical effect of obesity on the ventricular remodeling in adolescents with morbid obesity, and determined if subjects labelled as metabolically healthy obesity (MHO) presented better heart index than those with metabolically unhealthy obesity (MUO). Prospective case-control research of 45 adolescents (14-year-old) with morbid obesity and 25 normal weight adolescents' gender- and age-matched with Tanner stage 4-5. Left ventricle (LV) was evaluated by conventional Doppler echocardiography, tissue Doppler imaging and two-dimensional speckle tracking echocardiography. Compared to normal-weight subjects, adolescents with morbid obesity presented a high percentage of pathological LV geometry (87%; p<0.01), and systolic and diastolic dysfunctions only detected by E/A ratio (2.0 vs 1.7, p<0.01), global longitudinal strain (-21.0% vs -16.5%, p<0.01), and early diastolic strain rate (3.2 vs 2.2, p<0.01). A correlation was found between impaired cardiac index and body mass index (BMI), high blood pressure, hyperglycemia, low HDL-cholesterol and hypertriglyceridemia. BMI and HDL-cholesterol were the most significant independent variables. No significant differences were found in structural and functional cardiac index when MHO and MUO subjects were compared (global longitudinal strain: -17.0% vs -16.4%, p0.79). Morbidly obese adolescents have an abnormal LV geometry, closely related to BMI, and systolic and diastolic LV dysfunctions. Adolescents labelled as MHO, despite exhibiting better BMI and insulin-resistance values, present the same pathological heart changes as MUO. **(Am J Cardiol 2021;00:1−7)**

Pediatric obesity is the starting point for future health problems, so identifying subjects at significant risk is an urgent task to avoid future irreversible changes. Spain is one of the countries with the highest percentage of overweight and obese children in Europe (7-13 years old: 32%).[1] Metabolically healthy obese (MHO) subjects are characterized due to the lack of overt cardiometabolic abnormalities, while metabolically unhealthy obese (MUO) individuals present increased intra-abdominal fat mass, which predisposes to insulin-resistance and cardiometabolic events.[2,3] The estimated MHO prevalence among obese adolescents in Spain is 37%.[4] Unfortunately, there are few studies conducted in children with morbid obesity and the evaluation of myocardial index in MHO compared to MUO patients has been hardly evaluated.[5] Therefore, we sought to evaluate the preclinical effect of obesity on ventricular remodelling in adolescents with morbid obesity and determine if subjects labelled as MHO present a better heart index than those with MUO.

Methods

We studied 73 adolescents of both genders between 10 and 17 years old and Tanner's pubertal stage 4-5. Subjects with obesity were recruited from endocrinology clinics of participating hospitals and control participants were recruited from healthy volunteers in the cardiology and sports medicine clinics. Two groups were identified: the study group with morbid obesity (OG) (BMI-SD ≥4; n 48), and the control subjects (BMI 5-85 percentile, n 25) according to tables from the Barcelona Longitudinal Growth Study 1995−2017.[6] The control group adolescents were paired by age, gender and Tanner stage, with ratio 2 cases: 1 control, for minimizing the confounding effects.

Subjects with current infectious or recent acute inflammatory processes, history of prematurity or birth weight <2000 g, and smokers or those with pathologies that could change the arterial or myocardial wall– such as congenital heart disease, chronic kidney disease, transplant, rheumatic diseases, infection by HIV virus– were excluded. Considering that some subjects were recruited in the sports clinic, weekly sports hours were recorded. This potential confounding variable is poorly detailed in previous studies involving adolescents, although regular sports training duration and intensity can cause adaptive LV structural

[a]Hospital HM Nens. HM Hospitales, Barcelona, Spain; [b]Autonomous University of Barcelona, Spain; [c]Vall d'Hebron University Hospital, Barcelona, Spain; [d]CIBER of Rare Diseases (CIBERER) ISCIII, Spain; and [e]Biosfer Teslab − Metabolomics Platform, Rovira i Virgili University, Tarragona, Spain. Manuscript received May 5, 2021; revised manuscript received and accepted July 1, 2021.

Funding: JMS received grant funding for this project from the Spanish Society of Paediatric Cardiology and Congenital Heart Disease. DY used part of funds from "The Growth and Development group" (Vall d'Hebron Research Institute) partially financed for Novo Nordisk Pharma SA to finance the analysis of blood samples

See page 6 for disclosure information.

*Corresponding author: Tel: (34) 932-310-512.

E-mail address: jmsiurana@hotmail.com (J.M. Siurana).

0002-9149/
https://doi.org/10.1016/j.amjcard.2021.07.026

remodeling. An appropriate threshold of weekly sports hours was established according to some studies that defined a regular athlete when sports practice was more than 9 hours per week.[7] Hence, subjects that practiced >7 hours per week were not included in this study.

Written informed consent for participation was obtained and the Institutional Review Board at Vall d'Hebron Hospital approved the protocol (PR-AMI-273/2018). All subjects provided assent and informed consent had signed by their parents/legal guardians.

Demographic data of age, gender and clinical status were obtained from patient anamnesis. Blood pressure (BP) was obtained using a Welch Allyn Spot Vital Signs Monitor (4200B, Hillrom, Batesville, Indiana) after subjects had rested for 5 minutes, in a supine position and with an appropriately sized cuff giving measured mid-arm circumference, according to the criteria of the European Society of Hypertension.[8] In the same conditions, a 12-lead electrocardiogram was taken with a MAC 1200 ST (GE Healthcare's Clinical Systems, Chicago, USA). Recorded parameters were: heart rate, PR segment and corrected QT interval (Bazett's formula). Anthropometric measurements (weight, height) were obtained, and BMI (body weight divided by height in meters squared) and TMI (body weight divided by height in meters to the third power) were calculated.

EDTA blood samples were obtained at the time of enrollment at the participating hospitals in the morning after at least 8 hours of fasting. Samples for lipoprotein particle analysis were aliquoted, stored in liquid nitrogen (−80 °C) and dispatched on dry ice to Biosfer Teslab, where lipoprotein particle concentrations were measured by proton nuclear magnetic resonance spectroscopy, based on the LipoScale test.[9] Tests performed on blood samples in all subjects were: fasting glycemia and insulin, glycated haemoglobin, total cholesterol, cholesterol high-density lipoprotein (HDL-C), cholesterol low-density lipoprotein (LDL-C) and triglycerides (TG). An oral glucose tolerance test (OGTT) was undertaken only to OG, with the standard method (1.75 g/kg of body weight, up to a maximum of 75 g), measuring glucose and insulin serum levels at baseline and at 0, 30, 60, 90, and 120 min. Glucose intolerance and type 2 diabetes were diagnosed according to the criteria of the American Diabetes Association.[10] To evaluate insulin resistance, the homeostasis model assessment of insulin resistance (HOMA-IR) was calculated using the equation: fasting insulin (μU/ml) × fasting glucose (mmol/l)/22,5. Criteria to define MHO were based upon the expert consensus, which established that MHO subjects must comply with all of the following: HDL-cholesterol >40 mg/dl, triglycerides ≤150 mg/dl, systolic and diastolic blood pressure ≤90th percentile for age, gender, and height, and fasting glucose <100 mg/dl.[11] Although this definition excludes an evaluation of insulin-resistance, it is the most similar to accepted criteria in adults.[12]

Patients were examined using a Vivid S60 commercial ultrasound scanner (GE Vingmed Ultrasound AS, Horten, Norway) with a phased-array transducer (GE 3-MHz; GE Vingmed Ultrasound AS). Images were obtained at rest in the supine or left lateral decubitus position in the standard tomographic views of the LV (parasternal long and short axis and apical 4-chamber, 2-chamber, and long-axis views). All echocardiographic images were obtained prospectively by an experienced pediatric cardiologist, following the American Society of Echocardiography (ASE) guidelines.[13] LV diameter and wall thickness were measured from the 2-dimensional targeted M-mode echocardiographic tracing in two planes: parasternal long and short axis. LV end-diastolic (LVEDD) and end-systolic (LVESD) diameters and the LV ejection fraction (LVEF) were the average of the measurements in the two planes. Relative wall thickness (RWT) and LV mass were calculated using LV linear dimensions and following the recommendation of ASE.[13] The LV mass was determined by the adjusted Devereux's equation and the resultant value was indexed to height to the power of 2.7 (LVMI, g/m$^{2.7}$). Hypertrophy was considered when the LVMI value was above the 95th percentile for non-obese, healthy children >9 years old (>45 g/m$^{2.7}$ in males and >40 g/m$^{2.7}$ in females),[14] and LV geometry was categorized considering LVMI and RWT (0.41 is the 95th percentile) cutoff values.[15]

Using pulsed-wave Doppler, mitral inflow velocities (peak early diastolic velocity, peak late diastolic velocity, mitral E/A ratio, and isovolumic ventricular relaxation time) were measured. Tissue Doppler imaging was obtained by placing a 3.5 mm sample volume at the septal and lateral borders of the mitral annulus. Mean values of septal and lateral e' waves were obtained and the E/e' ratio was derived. S' wave was also measured in septal mitral annulus. Strain and strain rate were calculated according to the criteria of the ASE and the European Association of Cardiovascular Imaging.[16] Two-dimensional video loops were obtained for each patient in apical four, three, and two-chamber views, acquiring images at a frame rate of >65 frames/s. Offline image processing was performed using EchoPAC (version 204, GE Vingmed Ultrasound, Horten, Norway). After manually tracing along the endomyocardial border, the software automatically generated the epicardial border and the six segments, which were accepted after a visual inspection. To determine SR and midline strain, at least 17 out of 18 segments had to be included. Measured parameters were LV end-systolic GLS (%) and LV systolic and diastolic (early and late) longitudinal SR (1/sec). Resultant values were calculated by adding the strain of all accepted segments and dividing the value by the total number of segments.

Variability in the measurement of strain and SR, made by a single cardiologist, was evaluated in 10 randomly selected individuals by two observers (JMS, AS) for interobserver variability analysis. To determine the intraobserver reproducibility, the same observer repeated measurements for the 10 randomly selected patients at least four weeks later. The coefficient of variation (CV), defined as the ratio of the standard deviation and the absolute mean, was calculated for GLS and early and late diastolic SR. Additionally, the intraclass correlation coefficient (ICC) was estimated using Microsoft Excel Version 2016 (MS Excel 2016).

Data from the study were analyzed using descriptive statistics. Quantitative results were expressed as median and 25-75 interquartile range, while qualitative or dichotomous variables were expressed as percentages. Chi-square test (χ^2) and Fisher's exact test were used, according to the size

and characteristic of qualitative variables, to compare proportions and to study relationships between them. The non-parametric Mann-Whitney U test was used for comparison between two quantitative variables. To estimate correlations between parameters the Spearman's Rho correlation coefficient was calculated. A logistic regression was performed to model the probability of dichotomous events (normal or pathological LV geometry), and a multiple linear regression was made to determine relationships and dependence between independent and dependent (GLS and early diastolic SR) quantitative variables, which were significantly related by previous steps. Data were analyzed using IBM SPSS Statistics for Windows, version 23.0 (IBM Corp., Armonk, NY) and values of $p<0.05$ were considered significant.

Results

A total of 45 adolescents with obesity and 25 adolescents without obesity, adequately matched, were included in our study. Three subjects were excluded due to incomplete laboratory parameters or image data in the OG and none in the control group. Main clinical and laboratory data are expressed in Table 1. Both groups were well differenced in obesity index and significant differences were found in BP, insulin-resistance and dyslipidemia, while no differences were reported in Hb1Ac. In the group of adolescents with obesity, 33% were MHO subjects, 24% classified as glucose intolerance and 58% with systolic or diastolic high BP. No adolescent was diagnosed with type 2 diabetes mellitus in the OGTT. BP measurements showed a significant difference between both groups. The percentage of subjects with high BP in the OG was 58% for systolic BP and 27% for diastolic BP, while one control subject presented BP values above the 90th percentile (Fisher's exact test: systolic BP $p<0.01$, diastolic BP $p<0.01$).

Table 1
Characteristic, clinical and laboratory biochemistry data of study population

Variable	Control (n = 25)	Obese (n = 45)	p Value
Age (years)	14 [13−15]	14 [13−15]	0.99
Male	52%	38%	0.31
BMI (kg/m^2)	19.4 [17.8−22.1]	36.7 [34.5−39.8]	<0.01
BMI SD	−0.18 [−0.89 to 0.71]	7.4 [6.4−8.5]	<0.01
TMI (kg/m^3)	11.9 [10.8−12.6]	22.9 [20.9−25.2]	<0.01
Waist circumference (cm)	69 [65−74]	111 [103−120]	<0.01
SBP (mmHg)	108 [101−118]	125 [118−134]	<0.01
DBP (mmHg)	60 [60−68]	74 [66−79]	<0.01
HbA1c (%) (N=62)	5.2 [5.1−5.4]	5.3 [5.2−5.5]	0.16
HOMA-IR	1.2 [0.9−1.7]	4.7 [3.5−7.9]	<0.01
Total Cholesterol (mg/dL)	180 [164−191]	175 [151−196]	0.90
LDL-C (mg/dL)	102 [90−115]	105 [89−118]	0.81
HDL-C (mg/dL)	53 [48−61]	44 [40−49]	<0.01
Triglycerides (mg/dL)	77 [60−90]	99 [74−136]	<0.01
Obese phenotype	N/A	MHO	33%
		MUO	66%
OGTT	N/A	Normal	67%
		Intolerance	24%
		Type 2 DM	0%
		ND	9%
Sport (hours/week)	6 [5−6]	2 [1−2]	<0.01

Values expressed in median and 25%-75% IQR; P value calculated by T-test or non-parametric test (Mann-Whitney U test); Dichotomous variables (Fisher exact test); BMI, Body Mass Index; SD, Standard deviation; TMI, Tri-ponderal Mass Index; SBP, Systolic blood pressure; DBP, Diastolic blood pressure; HOMA-IR, Homeostatic model assessment insulin resistence; QUICKI, Quantitative Insulin Sensitivity Check Index; MUO, Metabolically unhealthy obesity; MHO, Metabolically healthy obesity; OGTT, Oral glucose tolerance test.

Electrocardiographic and structural and functional echocardiographic data are shown in Table 2. The most relevant structural change was detected in the LV geometry. A pathological geometry– defined as concentric remodeling, eccentric hypertrophy or concentric hypertrophy– was very common in OG. Significant differences in LV function were found in 2DSTE parameters, but no differences were observed when LVEF or tissue Doppler were used to evaluate the ventricular function.

An analysis between MHO and MUO in the OG was performed for previous heart measures (Table 3). No significant differences were demonstrated in structural and functional cardiac index. Moreover, when heart parameters of MHO subjects were compared with those of the control group, significant differences appeared in outstanding cardiac parameters.

Correlation analysis between demographic data and metabolic changes, and pathological geometry and 2DSTE parameters, are shown in Table 4. No correlation was found comparing MHO and MUO groups with the main structural and functional cardiac values.

Multivariable regression models were considered for GLS, early diastolic SR and LV pathological geometry. In the GLS final model ($R^2 = 0.42$, $p<0.0001$), independent determinants were BMI-SD (determinant coefficient: +50%, $p<0.01$) and HDL-cholesterol (determinant coefficient: -22%, $p<0.05$), while the final linear regression model of early diastolic SR ($R^2 = 0.26$, $p<0.0001$) had as independent parameter the BMI-SD (determinant coefficient: -52%, $p<0.01$). A binomial logistic regression was performed on LV pathological geometry, where the remaining independent parameter of the final model ($R^2 = 0.52$, $p<0.0001$) was BMI-SD (OR 2.2 [1.5-3.2], $p<0.01$).

The intra-observer and inter-observer variability analysis results for GLS and early diastolic SR measurements had a good reproducibility with CV of 16.9 and 18.8%, and 15.2 and 22.1%, respectively; and ICC of 0.98 and 0.92, and 0.97 and 0.95, respectively. Late diastolic SR obtained the poorest coefficients: CV 35.8%, 30.5%; and ICC 0.90, 0.94.

Discussion

This study demonstrated that morbidly obese adolescents presented a high percentage of pathological LV geometry, with eccentric hypertrophy being the most frequent, and systolic and diastolic dysfunctions only detected by strain techniques and mitral E/A ratio. Furthermore, BMI-SD and HDL-cholesterol were the most significant independent variables related to LV hypertrophy or remodeling and systolic dysfunction. Additionally, a correlation was found between impaired cardiac index and CVD risk factors. Finally, MHO patients showed no significant differences in

Table 2
Electrocardiographic data, M-mode echocardiography and functional parameters measured by conventional echocardiography, tissue Doppler and 2D Speckle Tracking echocardiography

Variable		Control	Obese	p Value
Heart Rate (bpm)		65 [59−74]	83 [72−92]	<0.01
PR Segment (ms)		130 [120−150]	130 [120−140]	0.29
QTc Interval (ms)		386 [359−398]	388 [377−400]	0.28
LVEDD (mm)		46 [44−49]	49 [46−51]	<0.01
LVESD (mm)		29 [27−31]	30 [27−31]	0.38
IVS (mm)		7.7 [7.1−8.5]	10.4 [9.2−11.1]	<0.01
LVPW (mm)		7.8 [6.8−8.5]	9.8 [8.4−10.5]	<0.01
LV Mass index (g/ht$^{2.7}$)		31 [26−33]	46 [43−54]	<0.01
RWT		0.33 [0.30−0.36]	0.40 [0.34−0.42]	<0.01
LV Geometry	Normal	96%	13%	<0.01
	CR	0%	11%	
	EH	4%	53%	
	CH	0%	22%	
LV Ejection Fraction (%)		68 [62−71]	69 [65−73]	0.58
Mitral E/A ratio		2.0 [1.7−2.5]	1.7 [1.4−1.9]	<0.01
IVRT (m/s)		52 [45−60]	50 [44−56]	0.20
Lateral E/e' ratio		7.6 [5.8−8.3]	6.8 [5.7−7.5]	0.10
Septal E/e' ratio		7.7 [6.9−8.3]	7.6 [7.2−8.4]	0.82
Septal S' (m/s)		0.08 [0.07−0.09]	0.09 [0.08−0.10]	0.06
GLS (%)		−21.0 [−23.2 to −19.2]	−16.5 [−18.3 to −14.3]	<0.01
Systolic GLSR (1/s)		−1.5 [−1.7 to −1.4]	−1.4 [−1.5 to −1.2]	<0.01
Early diastolic SR (1/s)		3.2 [2.8−3.3]	2.2 [1.9−2.5]	<0.01
Late diastolic SR (1/s)		0.67 [0.55−0.88]	0.70 [0.57−0.92]	0.40

Values expressed in median and 25%-75% IQR; P value calculated by T-test or non-parametric test (Mann-Whitney U test); Dichotomous variables (Chi-square test); LV, Left ventricle; RWT, Relative wall thickness; CR, Concentric remodeling; EH, Eccentric hypertrophy; CH, Concentric hypertrophy; IVRT, Isovolumic ventricular relaxation time; E/e', ratio of E wave mitral inflow by mean e'; Septal S', Systolic tissue Doppler velocity at septal mitral annulus; GLS, Global longitudinal strain; GLSR, Global longitudinal strain rate; SR, Strain rate.

structural and functional cardiac index when compared to MUO subjects.

Previous studies performed in the pediatric population also reported the eccentric LVH as the most common pathological geometry.[17,18] The larger abnormal LV geometry found in our OG (87%) could be explained because of the high values of BMI, similar to other studies.[18] Pathological LV geometry was correlated with elevated BP values, as in previous studies,[19] insulin-resistance and dyslipidemia (low HDL-cholesterol and high triglycerides), although the foremost independent determinant was BMI-SD. Electrocardiographic data did not show significant differences, although previous studies associated prolonged QTc intervals with the metabolic syndrome.[20]

Systolic and diastolic dysfunctions were evidenced in the OG by GLS and early diastolic SR, while classical evaluation methods, such as LVEF or tissue Doppler, did not reach pathological ranges. However, the mitral E/A ratio, as a marker of diastolic function, was significantly decreased in the OG. In correlation analysis, we found that HOMA-IR, systolic BP and HDL-cholesterol were highly correlated and diastolic BP and glycemia low correlated with deterioration in systolic strain and diastolic SR values. In multivariable analysis, BMI-SD was the final factor in systolic and diastolic strains and low HDL-cholesterol was also an independent variable for systolic dysfunction. Nevertheless, both analyses suggest the critical role of BP, insulin-resistance, glycemia and dyslipidemia on myocardial dysfunction in adolescents with morbid obesity. Multiple studies conducted in obese children and adolescents have demonstrated the relationship between BMI and global strain reduction, ranging from -14.6% to -18.4%.[21-23] However, few studies have been performed on the young population with severe obesity. In a published sub-cohort of 10 adolescents (BMI 41 kg/m^2), the mean GLS was -13.3%,[18] and in another study carried out in adolescents (BMI 36 kg/m^2), a mean GLS of -14.2% was reported.[24] In a large trial performed in young adults, the authors showed a mean GLS of -16.1% in the obese group vs -15.1% in the Type 2 Diabetes Mellitus group, and concluded that obesity alone is an independent predictor of reduced myocardial strain.[25] Our results showed longitudinal strain values similar to those published previously, especially in those studies conducted in severe obesity populations, and confirmed that BMI-SD and HDL-cholesterol are the foremost independent variables. The preload and afterload increase or the cardiac ectopic fat have been proposed as underlying mechanisms of the cardiac dysfunction.[26]

When MHO and MUO subjects were compared, we observed that subjects with morbid obesity labelled as healthy phenotype (without hypertension, dyslipidemia and hyperglycemia) exhibited less BMI value than those with the phenotype labelled as unhealthy. However, contrary to our expectations, no differences could be detected in the structural and functional cardiac damage. Although cardiac changes in childhood obesity have previously been associated with BP, insulin-resistance, glucose intolerance and dyslipidemia,[18,25] few studies directly compare both obesity phenotypes. One of these, conducted in children and adolescents with overweight and obesity, showed a significantly

Table 3
Differences in structural and functional cardiac parameters between metabolically healthy obesity (MHO) and metabolically unhealthy obesity (MUO) phenotypes

Variable	Control (n = 25)	Obese (n = 45)		p Value		
		MHO (n = 15)	MUO (n = 30)	Control vs Obese	Control vs MHO	MHO vs MUO
Age (years)	14 [13–15]	14 [13–16]	14 [13–15]	0.99	0.80	0.61
BMI (kg/m^2)	19.4 [17.8–22.1]	35.2 [32.8–37.9]	37.2 [35.6–42.0]	<0.01	<0.01	0.02
BMI SD	-0.18 [-0.89–0.71]	7.1 [6.0–8.2]	7.7 [6.6–9.6]	<0.01	<0.01	0.11
TMI (kg/m^3)	11.9 [10.8–12.6]	22.9 [20.6–24.3]	22.7 [20.9–25.9]	<0.01	<0.01	0.44
SBP (mmHg)	108 [101–118]	118 [113–120]	130 [123–140]	<0.01	0.05	<0.01
DBP (mmHg)	60 [60–68]	68 [63–74]	76 [68–83]	<0.01	0.10	<0.01
HbA1c (%) (N=62)	5.2 [5.1–5.4]	5.3 [5.2–5.4]	5.4 [5.2–5.6]	0.16	0.58	0.22
HOMA-IR	1.2 [0.9–1.7]	3.8 [2.7–5.1]	6.3 [3.6–8.9]	<0.01	<0.01	0.03
Total Cholesterol (mg/dL)	180 [164–191]	172 [146–195]	176 [163–197]	0.90	0.72	0.63
LDL-C (mg/dL)	102 [90–115]	110 [84–117]	105 [91–120]	0.81	0.91	0.63
HDL-C (mg/dL)	53 [48–61]	45 [42–51]	42 [38–48]	<0.01	<0.01	0.09
Triglycerides (mg/dL)	77 [60–90]	91 [65–123]	108 [76–154]	<0.01	0.07	0.17
Sport (hours/week)	6 [5–6]	2 [2–4]	2 [1–2]	<0.01	<0.01	0.51
Heart Rate (bpm)	65 [59–74]	83 [69–92]	83 [72–93]	<0.01	<0.01	0.41
PR Segment (ms)	130 [120–150]	120 [100–130]	130 [100–140]	0.29	0.07	0.08
QTc Interval (ms)	386 [359–398]	384 [376–406]	389 [379–399]	0.28	0.34	0.89
LV Mass index (g/ht$^{2.7}$)	31 [26–33]	46 [43–51]	46 [42–57]	<0.01	<0.01	0.66
RWT	0.33 [0.30–0.36]	0.38 [0.33–0.41]	0.41 [0.35–0.44]	<0.01	<0.01	0.20
LV Geometry Normal	96%	6%	17%	<0.01	<0.01	0.09
CR	0%	6%	13%			
EH	4%	80%	40%			
CH	0%	6%	30%			
LV Ejection Fraction (%)	68 [62–71]	68 [65–74]	69 [63–72]	0.58	0.52	0.72
Mitral E/A ratio	2.0 [1.7–2.5]	1.7 [1.4–1.9]	1.6 [1.4–1.9]	<0.01	<0.01	0.66
IVRT (m/s)	52 [45–60]	47 [45–52]	50 [42–58]	0.20	0.15	0.32
Lateral E/e' ratio	7.6 [5.8–8.3]	6.8 [5.7–7.5]	6.7 [5.6-7.7]	0.10	0.19	0.80
Septal E/e' ratio	7.7 [6.9–8.3]	7.6 [7.4–8.3]	7.5 [7–8.6]	0.82	0.61	0.32
Septal S' (m/s)	0.08 [0.07–0.09]	0.08 [0.07–0.09]	0.09 [0.08–0.11]	0.06	0.63	0.02
GLS (%)	−21.0 [-23.2 to -19.2]	−17.0 [-18.4 to -13.8]	−16.4 [−18.3 to -14.6]	<0.01	<0.01	0.79
Systolic GLSR (1/sec)	−1.5 [-1.7 to -1.4]	−1.4 [-1.5 to -1.2]	−1.4 [−1.5 to −1.3]	<0.01	<0.01	0.27
Early diastolic SR (1/sec)	3.2 [2.8–3.3]	2.2 [2.0–2.4]	2.2 [1.9–2.6]	<0.01	<0.01	0.61
Late diastolic SR (1/sec)	0.67 [0.55–0.88]	0.66 [0.56–0.73]	0.72 [0.57–0.97]	0.40	0.80	0.16

Median and 25%-75% IQR, Non-parametric test (Mann-Whitney U test); Dichotomous variables (Chi-square test); BMI, Body Mass Index; SD, Standard deviation; TMI, Tri-ponderal Mass Index; HOMA-IR, Homeostatic model assessment insulin resistence; LV, Left ventricle; RWT, Relative wall thickness; CR, Concentric remodeling; EH, Eccentric hypertrophy; CH, Concentric hypertrophy; IVRT, Isovolumic ventricular relaxation time; E/e', ratio of E wave mitral inflow by mean e'; Septal S', Systolic tissue Doppler velocity at septal mitral annulus; GLS, Global longitudinal strain; GLSR, Global longitudinal strain rate; SR, Strain rate.

worse GLS among MUO patients compared to MHO (-17.3 vs -19.1%),[5] although different criteria were used to define MHO. Our study showed no significant differences, but a worse tendency in MUO subjects. In light of our results, an explanation could be that, although catalogued as MHO, adolescents in the morbid range of obesity continue presenting impaired cardiac index even before reaching pathological levels in BP, glycemia or lipid profile in a preclinical and preanalytical stage. It is also possible that some of MHO subjects will probably progress to MUO in a few years, as previous studies have documented.[27]

This study has some limitations, such as its cross-sectional design and the small sample size, especially in the control group, although it was well matched by age, gender and Tanner stage. Therefore, the GLS value of our control group is similar to the 2DSTE analysis published in a meta-analysis carried out in the pediatric population.[28] Additionally, the absence of radial and circumferential deformation measurements could also be considered as a limitation. However, the poor quality of the echocardiographic acoustic window in morbidly obese subjects, especially in the parasternal short-axis 2D view, made the authors decide not to record these measurements. The GLS value has demonstrated a higher accuracy than circumferential strain in normal hearts and is the strain value most often associated with higher mortality rates in at-risk populations.[29,30]

In conclusion, adolescents with morbid obesity have an abnormal LV geometry, closely related to BMI values, and systolic and diastolic LV dysfunctions, even when primary comorbidities, such as diabetes mellitus, have not yet been diagnosed. Furthermore, those adolescents labelled as MHO, despite exhibiting better BMI, BP, insulin-resistance and lipid profile, present the same pathological heart changes as MUO. Therefore, omitting cardiac evaluation for any adolescent with morbid obesity misses the opportunity to identify early cardiac damage. However, investigations with long-term follow-up are necessary for pediatric populations with morbid obesity to determine if changes

Table 4
Correlated parameters with LV pathological geometry, systolic (GLS) and diastolic (early diastolic SR) functions

	Pathological Geometry	GLS	Early diastolic SR
Age	0.10	0.09	-0.28*
Gender (male)	-0.10	0.04	-0.12
BMI	0.66**	0.61**	-0.65**
BMI SD	0.66**	0.61**	-0.64**
TMI	0.67**	0.61**	-0.60**
Waist circumference	0.67**	0.60**	-0.69**
Systolic BP	0.40**	0.46**	-0.45**
Diastolic BP	0.31**	0.37**	-0.28*
Fasting plasma glucose	0.28*	0.35*	-0.36**
HOMA-IR	0.58**	0.60**	-0.47**
Total Cholesterol	0.11	-0.05	0.06
LDL-cholesterol	0.00	0.01	0.06
HDL-cholesterol	-0.32**	-0.51**	0.55**
Triglycerides	0.33**	0.25*	-0.22

Values expressed in r.

GLS, Global longitudinal strain; SR, Strain rate; BMI, Body Mass Index; TMI, Tri-ponderal Mass Index; HOMA-IR; Homeostatic model assessmen insulin resistence; BP, Blood presure.

* $p<0.05$.

** $p<0.01$.

observed in ventricular structure and function result in future cardiovascular events.

Acknowledgements

The authors wish to acknowledge the work of Dr. Ariadna Campos from Vall d'Hebron Hospital, and Dr. Georges Akel and Dr. Zelmira Bosch from HM Nens Hospital. We also wish to thank Dr. Roser Ferrer from the biochemistry department of Vall d'Hebron Hospital and Dr. Eduard Furnells from Duran Bellido Laboratory. The project was funded by the Spanish Society of Paediatric Cardiology and Congenital Heart Disease and partially funded by "The Growth and Development group" (Vall d'Hebron Research Institute).

Disclosures

The authors declared no conflict of interest.The authors declare the following financial interests/personal relationships which may be considered as potential competing interests: Jose M. Siurana reports financial support was provided by Spanish Society of Paediatric Cardiology and Congenital Heart Disease. Diego Yeste reports financial support was provided by Vall d'Hebron Research Institute.

1. Garrido-Miguel M, Cavero-Redondo I, Álvarez-Bueno C, Rodríguez-Artalejo F, Moreno LA, Ruiz JR, Ahrens W, Martínez-Vizcaíno V. Prevalence and trends of overweight and obesity in European children from 1999 to 2016: a systematic review and meta-analysis. *JAMA Pediatr* 2019;173:e192430.
2. Blüher M. Metabolically healthy obesity. *Endocr Rev* 2020;41:405–420.
3. Eckel N, Meidtner K, Kalle-Uhlmann T, Stefan N, Schulze MB. Metabolically healthy obesity and cardiovascular events: a systematic review and metanalysis. *Eur J Prev Cardiol* 2016;23:956–966.
4. Yeste D, Clemente M, Campos A, Fábregas A, Mogas E, Soler L, Carrascosa A. Diagnostic accuracy of the tri-ponderal mass index in identifying the unhealthy metabolic obese phenotype in obese patients. *An Pediatr (Barc)* 2021;94:68–74.
5. Corica D, Oreto L, Pepe G, Calabro MP, Longobardo L, Morabito L, Pajno GB, Alibrandi A, Aversa T, Wasniewska M. Precocious preclinical cardiovascular sonographic markers in metabolically healthy and unhealthy childhood obesity. *Front Endocrinol (Lausanne)* 2020;11:56.
6. Carrascosa A, Yeste D, Moreno-Galdó A, Gussinyé M, Ferrández A, Clemente M, Fernández-Cancio M. Body mass index and tri-ponderal mass index of 1,453 healthy non-obese, non-undernourished millennial children. The Barcelona longitudinal growth study. *An Pediatr (Bar)* 2018;89:137–143.
7. Prakken NH, Velthuis BK, Teske AJ, Mosterd A, Mali WP, Cramer MJ. Cardiac MRI reference values for athletes and nonathletes corrected for body surface area, training hours/week and sex. *Eur J Cardiovasc Prev Rehabil* 2010;17:198–203.
8. Lurbe E, Agabiti-Rosei E, Cruickshank JK, Dominiczak A, Erdine S, Hirth A, Invitti C, Litwin M, Mancia G, Pall D, Rascher W, Redon J, Schaefer F, Seeman T, Sinha M, Stabouli S, Webb NJ, Wühl E, Zanchetti A. 2016 European Society of Hypertension guidelines for the management of high blood pressure in children and adolescents. *J Hypertens* 2016;34:1887–1920.
9. Mallol R, Amigó N, Rodríguez MA, Heras M, Vinaixa M, Plana N, Rock E, Ribalta J, Yanes O, Masana L, Correig X. Liposcale: a novel advanced lipoprotein test based on 2D diffusion-ordered 1H NMR spectroscopy. *J Lipid Res* 2015;56:737–746.
10. Association American Diabetes. Classification and diagnosis of diabetes. *Diabetes Care* 2017;40(Suppl.1):S11–S24.
11. Damanhoury S, Newton AS, Rashid M, Hartling L, Byrne JLS, Ball GDC. Defining metabolically healthy obesity in children: a scoping review. *Obes Rev* 2018;19:1476–1491.
12. Lavie CJ, Laddu D, Arena R, Ortega FB, Alpert MA, Kushner RF. Healthy weight and obesity prevention: JACC health promotion series. *J Am Coll Cardiol* 2018;72:1506–1531.
13. Chamber Quantification Writing Group; American Society of Echocardiography's Guidelines and Standards Committee; European Association of Echocardiography, Lang RM, Bierig M, Devereux RB, Flachskampf FA, Foster E, Pellikka PA, Picard MH, Roman MJ, Seward J, Shanewise JS, Solomon SD, Spencer KT, Sutton MS, Stewart WJ. Recommendations for chamber quantification: a report from the american society of echocardiography's guidelines and standards committee and the chamber quantification writing group, developed in conjunction with the European Association of Echocardiography, a branch of the European Society of Cardiology. *J Am Soc Echocardiogr* 2005;18:1440–1463.
14. Khoury PR, Mitsnefes M, Daniels SR, Kimball TR. Age-specific reference intervals for indexed left ventricular mass in children. *J Am Soc Echocardiogr* 2009;22:709–714.
15. Daniels SR, Loggie JM, Khoury P, Kimball TR. Left ventricular geometry and severe left ventricular hypertrophy in children and adolescents with essential hypertension. *Circulation* 1998;97:1907–1911.
16. Voigt JU, Pedrizzetti G, Lysyansky P, Marwick TH, Houle H, Baumann R, Pedri S, Ito Y, Abe Y, Metz S, Song JH, Hamilton J, Sengupta PP, Kolias TJ, d'Hooge J, Aurigemma GP, Thomas JD, Badano LP. Definitions for a common standard for 2D speckle tracking echocardiography: consensus document of the EACVI/ASE/Industry Task Force to standardize deformation imaging. *J Am Soc Echocardiogr* 2015;28:183–193.
17. Di Bonito P, Moio N, Sibilio G, Cavuto L, Sanguigno E, Forziato C, de Simone G, Capaldo B. Cardiometabolic phenotype in children with obesity. *J Pediatr* 2014;165:1184–1189.
18. Sanchez AA, Levy PT, Sekarski TJ, Arbelaez AM, Hildebolt CF, Holland MR, Singh GK. Markers of cardiovascular risk, insulin resistance, and ventricular dysfunction and remodelling in obese adolescents. *J Pediatr* 2015;166:660–665.
19. Pieruzzi F, Antolini L, Salerno FR, Giussani M, Brambilla P, Galbiati S, Mastriani S, Rebora P, Stella A, Valsecchi MG, Genovesi S. The role of blood pressure, body weight and fat distribution on left ventricular mass, diastolic function and cardiac geometry in children. *J Hypertens* 2015;33:1182–1192.
20. Guo X, Li Z, Guo L, Yu S, Yang H, Zheng L, Pan G, Zhang Y, Sun Y, Pletcher MJ. Effects of metabolically healthy and unhealthy obesity

on prolongation of corrected QT interval. *Am J Cardiol* 2017;119: 1199–1204.
21. Kibar AE, Pac FA, Ece İ, Oflaz MB, Ballı Ş, Bas VN, Aycan Z. Effect of obesity on left ventricular longitudinal myocardial strain by speckle tracking echocardiography in children and adolescents. *Balkan Med J* 2015;32:56–63.
22. Barbosa JA, Mota CC, Simões AC, Nunes MC, Barbosa MM. Assessing preclinical ventricular dysfunction in obese children and adolescents: the value of speckle tracking imaging. *Eur Heart J Cardiovasc Imaging* 2013;14:882–889.
23. Mangner N, Scheuermann K, Winzer E, Wagner I, Hoellriegel R, Sandri M, Zimmer M, Mende M, Linke A, Kiess W, Schuler G, Körner A, Erbs S. Childhood obesity: impact on cardiac geometry and function. *JACC Cardiovasc Imaging* 2014;7:1198–1205.
24. Obert P, Gueugnon C, Nottin S, Vinet A, Gayrard S, Rupp T, Dumoulin G, Tordi N, Mougin F. Two-dimensional strain and twist by vector velocity imaging in adolescents with severe obesity. *Obesity (Silver Spring)* 2012;20:2397–2405.
25. Haley JE, Zhiqian G, Philip KR, Nicolas ML, Thomas KR, Lawrence DM, Elaine UM. Reduction in myocardial strain is evident in adolescents and young adults with obesity and type 2 diabetes. *Pediatr Diabetes* 2020;21:243–250.
26. Cote AT, Harris KC, Panagiotopoulos C, Sandor GG, Devlin AM. Childhood obesity and cardiovascular dysfunction. *J Am Coll Cardiol* 2013;62:1309–1319.
27. Eckel N, Li Y, Kuxhaus O, Stefan N, Hu FB, Schulze MB. Transition from metabolic healthy to unhealthy phenotypes and association with cardiovascular disease risk across BMI categories in 90 257 women (the Nurses' Health Study): 30 year follow-up from a prospective cohort study. *Lancet Diabetes Endocrinol* 2018;6:714–724.
28. Levy PT, Machefsky A, Sanchez AA, Patel MD, Rogal S, Fowler S, Yaeger L, Hardi A, Holland MR, Hamvas A, Singh GK. Reference ranges of left ventricular strain measures by two-dimensional speckle-tracking echocardiography in children: a systematic review and meta-analysis. *J Am Soc Echocardiogr* 2016;29:209–225.
29. Singh GK, Cupps B, Pasque M, Woodard PK, Holland MR, Ludomirsky A. Accuracy and reproducibility of strain by speckle tracking in pediatric subjects with normal heart and single ventricular physiology: a two-dimensional speckle-tracking echocardiography and magnetic resonance imaging correlative study. *J Am Soc Echocardiogr* 2010;23:1143–1152.
30. Patel MD, Myers C, Negishi K, Singh GK, Anwar S. Two-dimensional strain is more precise than conventional measures of left ventricular systolic function in pediatric patients. *Pediatr Cardiol* 2020;41:186–193.

6. LIPOPROTEIN PARTICLE PROFILES AND CARDIAC INVOLVEMENT STUDY

6.1 Introduction

Obesity is a multifactorial disease that includes several preceding disorders of CVD, such as high BP, insulin resistance, diabetes and dyslipidemia. However, the majority of obese children present a pre-pathological condition, therefore identifying which of them are at increased risk of developing CVD is a challenge for pediatricians.

In the conventional lipid profile, the increase in LDL-C has been demonstrated as one of the most important factors associated with CVD risk,[1] but the role of HDL-C or TG remains unclear.[2] Additionally, the remnant cholesterol – a derivative from the CLP that accounts for the cholesterol enclosed in the VLDL, IDL and chylomicrons – has been also associated with increased prevalence of ischemic heart disease and myocardial infarction.[3,4] On the other hand, the advanced lipoprotein testing, assessed by proton nuclear magnetic resonance spectroscopy of plasma, provides much information about lipoprotein characteristics as it quantifies the concentration, particle size and composition (cholesterol or TG) of each lipoprotein subclass. Previous studies have shown how in situations of apparent normality, specific lipoprotein alterations are highly associated with future CVD events.[5-8] Thus, the concept of atherogenic

dyslipidemia – applied to subjects with hypo HDL-C, hypertriglyceridemia and normal LDL-C, but increases in some ALT components – has been associated with an elevated risk of CVD events.[9-11]

Various studies have evaluated the ALT in obese adults and adolescents and established its utility in predicting arterial wall changes, coronary heart disease or CVD events,[12-14] however to our knowledge, none have analyzed which ALT components are closely associated with cardiac changes in obese adolescents. The objective of the current study is to evaluate the ALT and its relationship with cardiac changes, metabolic syndrome (MS) and inflammatory markers in the same cohort of morbidly obese adolescents with normal CLP and without type 2 diabetes mellitus (T2-DM), the most common scenario in obese adolescents.

6.2 Methodology

6.2.1 Study Population

We studied 67 adolescents of both genders between 10 and 17 years old. Subjects with morbid obesity were recruited from endocrinology clinics and control participants were recruited from healthy volunteers in the cardiology and sports medicine clinics.

Subjects with current infectious or recent acute inflammatory processes, history of prematurity or birth weight <2000 g, and smokers or those whose pathologies could affect the cardiovascular system – such as congenital heart disease, chronic kidney disease, transplant, rheumatic diseases, and HIV infection – were excluded. Similarly,

obese subjects with T2-DM and control subjects who practiced >7 weekly sport hours, a threshold explained in our previous study,[15] were also excluded in this analysis.

Subjects were classified depending on the degree of cardiac involvement and three groups were established: no cardiac changes (n = 25), formed by control and obese adolescents without LV changes; mild cardiac changes (n = 17), consisting of 15 obese adolescents with LV remodeling and 2 control adolescents with border systolic dysfunction; and severe cardiac changes (n = 25), constituted by morbidly obese adolescents with LV remodeling and systolic dysfunction, based on the threshold below defined. For the second analysis, subjects were reclassified according to their BMI, calculated from tables of the Barcelona Longitudinal Growth Study 1995–2017,[16] in two groups: subjects with morbid obesity (SDS-BMI ≥4; n = 42), and with normal weight (BMI 5th-85th percentile, n = 25). Finally, the last classification of subjects was performed on the base of MS criteria from Cook et al,[17] identifying two groups: subjects without MS (n = 53), and with MS (n = 14).

Written informed consent for participation was obtained and the Institutional Review Board at Vall d'Hebron Hospital approved the protocol (PR-AMI-273/2018). All subjects provided assent and an informed consent was signed by their parents/legal guardians.

6.2.2 Clinical and Laboratory Assessment

Demographic data of age, gender and clinical status were obtained from patient anamnesis. Blood pressure was obtained using a Welch Allyn Spot Vital Signs Monitor

(4200B, Hillrom, Batesville, Indiana) after subjects had rested for 5 minutes, in a supine position and with an appropriately sized cuff giving measured mid-arm circumference, according to the criteria of the European Society of Hypertension,[18] which also defines the high BP values by age and gender.

EDTA blood samples were obtained at the time of enrollment at the participating hospitals in the morning after at least 8 hours of fasting. Samples for lipoprotein particle analysis were aliquoted, stored in liquid nitrogen (−80°C) and shipped on dry ice to Biosfer Teslab, where the ALT was measured by 1H-NMR spectroscopy, based on the LipoScale test®.[19] For each main lipoprotein class (VLDL, LDL and HDL) we obtained large, medium and small subclass particle concentrations, mean particle size and composition. Additionally, tests performed on blood samples from all subjects were: fasting glycemia and insulin, glycated hemoglobin and the CLP (total cholesterol, HDL-C, LDL-C and TG). To evaluate insulin resistance, the homeostasis model assessment of insulin resistance (HOMA-IR) was calculated using the equation: fasting insulin (µU/ml) × fasting glucose (mmol/l) / 22.5. Inflammation markers evaluated were highly-sensitive C-reactive protein (hs-CPR) and an NMR derived glycoprotein biomarker, termed GlycA, arising from the concentration of the acetyl groups of N-acetylglucosamine and N-acetylgalactosamine bond to plasmatic proteins. Glyc A is able to detect low-grade chronic inflammation in obesity and insulin resistance's disorders,[20-22] and in atherosclerosis progression.[23]

6.2.3 Echocardiographic Image Acquisition and Analysis

Patients were examined using a Vivid S60 commercial ultrasound scanner (GE Vingmed Ultrasound AS, Horten, Norway) with a phased-array transducer (GE 3-MHz; GE Vingmed Ultrasound AS). Images were obtained at rest in the supine or left lateral decubitus position in the standard tomographic views of the LV (parasternal long and short axis and apical 4-chamber, 2-chamber, and long-axis views). All echocardiographic images were obtained prospectively by an experienced pediatric cardiologist, according to the criteria of the American Society of Echocardiography (ASE).[24]

To evaluate the LV geometry, relative wall thickness (RWT) and LV mass were calculated using LV linear dimensions and following the recommendation of ASE.[24] The LV mass was determined by the adjusted Devereux's equation and the resultant value was indexed to height to the power of 2.7 (LVMI, $g/m^{2.7}$). LV geometry was categorized as normal or pathological (concentric remodeling, eccentric hypertrophy and concentric hypertrophy) considering the following cutoff values (95^{th} percentile in the pediatric population): LVMI >45 $g/m^{2.7}$ in males and >40 $g/m^{2.7}$ in females,[25] and RWT >0.41.[26]

The LV function was determined by two-dimensional speckle tracking echocardiography, a well-validated and precise method to quantify ventricular function with lower variability than LV ejection fraction in pediatric patients.[27] Strain and strain rate (SR) were calculated according to the criteria of the ASE[24] and the European Association of Cardiovascular Imaging.[27] Two-dimensional video loops were obtained for each patient in apical four, three, and two-chamber views, acquiring images at a frame rate of >65 frames/s. Offline image processing was performed using EchoPAC (version 11.2, GE Vingmed Ultrasound, Horten, Norway). After manually tracing along

the endomyocardial border, the software automatically generated the epicardial border and the six segments, which were accepted after a visual inspection. To determine SR and midline strain, at least 17 out of 18 segments had to be included. Measured parameters were LV end-systolic global longitudinal strain (GLS, %) and LV early diastolic global longitudinal SR (early GLSR, 1/sec). Resultant values were calculated by adding the strain of all accepted segments and dividing the value by the total number of segments. The GLS cutoff value which defined systolic dysfunction in this study was -16.7%, which corresponds to the lowest GLS value reported in a meta-analysis of LV strain measures by echocardiography in children.[28]

6.2.4 Statistical Analysis

Data from the study were analyzed using descriptive statistics. Quantitative results were expressed as median and 25-75 interquartile range, while qualitative or dichotomous variables were expressed as percentages. Chi-square test (χ^2) and Fisher's exact test were used, according to the size and characteristic of qualitative variables, to compare proportions and to study relationships between them. The comparison between two quantitative variables was made by the nonparametric Mann-Whitney U test. To estimate correlations between parameters, the Pearson and Spearman's Rho correlation coefficients were calculated as appropriate for the type of the data. Data was analyzed by using IBM SPSS Statistics for Windows, version 23.0 (IBM Corp., Armonk, N.Y.) and values of $p<0.05$ were considered significant.

A three-step multivariate analysis was applied to identify important variables and patterns that allowed distinguishing between the three cardiac involvement

groups. In the first step, we applied three statistical approaches to identify the variables that make the largest contributions to the discrimination between groups. These approaches include the Wilcoxon rank-sum test, the Random Forest, and the Partial Least Squares discriminant analysis (PLS-DA). Those variables that resulted significant with a p-value <0.05 were selected as the candidate for the Wilcoxon rank-sum test, and the 5-10 most important variables were determined by the variable importance score or the variable importance in projection (VIP) score using the Random Forest or the PLSA-DA, respectively. To avoid overfitting, 10-fold cross-validation was performed. In the second step, by using a Venn diagram we selected the most prominent variables and those that will be included in the model by determining those that overlap by the statistical approaches. In the third step, we used the Principal Component Analysis (PCA) as an unsupervised method to visualize the capacity of the selected variables to drive group separation. Ellipses in PCA represent 90% confidence intervals around the centroid of each data cluster. Finally, we built a linear fitting model, and by computing the area under the curve (AUC) and the 95% confidence interval of a receiver operating characteristics (ROC) curve we evaluated and quantified how accurately the selected variables were able to discriminate between groups. Patients were randomly assigned to training (60%) and test (40%) sets. We performed 10-fold cross-validation with 100 replicates on the training data during the model construction process and tested the model on the hold-out data. Analysis was performed using the R statistical software version 4.1.1 (Chapman & Hall/CRC Computational Biology Series).

6.3 Results

A total of 42 adolescents with obesity and 25 adolescents without obesity, age-matched, were included in our study. No subject was excluded, although HbA1c was not registered in ten subjects of the obese group and hs-CPR values were missed in one control and three obese subjects. Main clinical, laboratory and echocardiographic data from the three cardiac groups are summarized in Table 1. No significant differences were noted in age, but most obese subjects were classified in the mild or severe cardiac change groups. However, the significant increase observed in BP, HOMA-IR and inflammation markers among the three groups suggests a relationship between the severity of cardiac changes and the worsening in CV risk factors, except in the conventional lipid profile, where no differences were found among both groups with cardiac changes. In contrast, significant differences were detected in the ALT (Table 1), and a pathological phenotype related to cardiac changes was defined (Figure 1): increases in concentrations of total VLDL-P, large VLDL-P, total LDL-P, small LDL-P, ratio LDL-P/HDL-P, and HDL lipid composition (ratio HDL-TG/HDL-C), and decreases in concentrations of total HDL-P and medium HDL-P, and in the LDL size.

Data of LV geometry and speckle tracking determinations from the echocardiographic evaluation are summarized in Supplemental Table S1.

Table 2 shows the clinical characteristics, laboratory parameters and ALT of subjects classified by obesity index. The obese subjects exhibited, in addition to the pathological ALT phenotype observed in subjects with cardiac changes, a mild, though significant, difference in the concentration of HDL-C (52 vs 44 mg/dL, $p<0.01$), triglycerides (77 vs 91 mg/dL, $p<0.01$) and remnant cholesterol (19.1 vs 23.9 mg/dL,

p0.01) (Figure 1). Finally, data of subjects categorized by MS criteria are summarized in Table 3. Obese adolescents who accomplished MS criteria showed overall worse BP, insulin resistance and hs-CPR values than any of the previous groups. Their CLP was characterized by marked differences in triglycerides (78 vs 124 mg/dL, $p<0.01$) and remnant cholesterol (19.6 vs 30.3 mg/dL, $p<0.01$), while the ALT was characterized by significant increases in: total VLDL-P, large VLDL-P, ratio LDL-P/HDL-P and HDL lipid composition (ratio HDL-TG/HDL-C) (Figure 1).

Correlation analysis between ALT components and variables of LV geometry and function, HOMA-IR and inflammatory markers are summarized in Table 4. The ratios LDL-P/HDL-P and HDL-TG/HDL-C were the variables better correlated to cardiac changes as well as to insulin resistance and inflammation parameters. Moreover, considering the specific subclasses of lipoprotein particles, the results indicated that large VLDL-P, small LDL-P and total HDL-P (inversely) subclasses have the best correlation to LV remodeling and systo-diastolic dysfunction, while lipoprotein particles rich in triglycerides (VLDL-P and TG-enriched HDL) had the highest association with HOMA-IR. Lastly, total HDL-P and small LDL-P were particles related with hs-CPR values, whereas GlycA proved to be better correlated with every component of the ALT, so this inflammatory marker was chosen for the multivariable analysis. Correlation analysis between ALT and CLP components are summarized in Supplemental Table S2. Triglycerides appeared particularly associated with VLDL-P and large HDL-P.

The final multivariable model with the largest AUC (0.79 [95% CI: 0.54-1]) for distinguishing mild cardiac change subjects from those with severe cardiac changes identified the following pattern: HOMA-IR, GlycA, VLDL-diameter and large HDL-P

(Figure 2). In contrast, for differentiating normal heart subjects from those with severe cardiac changes the largest AUC (0.91 [95% CI: 0.74-1]) resulted from the following variables: BMI standard deviation, HOMA-IR, systolic BP, diastolic BP, GlycA, small VLDL-P, small LDL-P and ratio HDL-TG/HDL-C (Figure 3). Additionally, ROC curves with only traditional CV risk factors (BMI standard deviation, HOMA-IR, systolic and diastolic BP) were developed to assess the usefulness of lipoprotein subclasses and glycoprotein A in the multivariable diagnostic model. Figure 4 shows the comparative ROC curve analysis.

Reproducibility of echocardiographic parameters has been demonstrated previously, showing good intraclass correlation coefficients.[15]

6.4 Discussion

This study showed that morbidly obese adolescents with LV changes presented a pathological phenotype in the ALT despite exhibiting normal values in the CLP (Figure 1). Large VLDL-P, small LDL-P and total HDL-P were the subclasses more closely related to cardiac changes, while ratios which highlighted the excess of VLDL-P and LDL-P in relation to HDL-P appeared to be the variables more closely associated with severity in the LV changes. Furthermore, when obese adolescents were classified by MS criteria or obesity index, the resulting ALT was determined by the high triglyceridemia of these subjects, and hence, predominated TG-enriched lipoproteins, like VLDL and TG-enriched HDL (Figure 1). Additionally, the inflammatory markers exhibited a correlation with the aforementioned pathological ALT and especially with lower levels of total HDL-P and an altered LDL subclass distribution, moved to the smallest LDL

subclass. Finally, multivariable models showed the relevance of VLDL-diameter and large HDL-P — as well as BP, insulin resistance and inflammation — in the changes observed in obese adolescent's hearts. Our results have highlighted the importance of ALT and GlycA as differentiating indicators of cardiac severity in adolescents with a similar degree of obesity, where minimum differences exist in BMI, BP or insulin resistance levels.

Previous studies performed in obese or diabetic children have shown similar results. Thus, the most frequently reported ALT was defined by increases of small LDL-P and VLDL-P and decreases of LDL size and large-medium HDL-P.[12,29-31]

VLDL are the main carriers of plasmatic triglycerides, and hence appear particularly increased in subjects with hypertriglyceridemia. In contrast, LDL are cholesterol-enriched lipoproteins and their concentration is not so triglyceride-dependent, however in hypertriglyceridemia conditions the LDL particles have been found to be smaller and compositionally cholesterol-depleted.[32] The small LDL subclass possesses an increased atherogenicity – on account of mechanisms like endothelial barrier crossing facility or oxidation susceptibility[32] – and it has been postulated as a predictor risk factor for coronary heart disease.[33] Similarly, the relevance of LDL-P concentration to predict future CVD events rather than LDL-C has been also documented in the Framingham Offspring Study,[5] where the highest risk was attributed to subjects with high LDL-P and low LDL-C. Our study, performed in a population with low LDL-C, has shown a significant increase in the small LDL subclass in the obese group. Additionally, in the descriptive statistics, the latter seemed to be the best differentiating lipoprotein subclass between subjects with severe cardiac changes

and those with mild or no cardiac changes, having been found to be correlated with LV remodeling, systo-diastolic dysfunction, insulin resistance and inflammation. Concerning triglyceride levels, a strong positive correlation was found with all VLDL subclasses and large HDL-P, but apparently, their levels were independent of the small LDL-P subclass, as reported in the Framingham Offspring Study. Regarding VLDL-P, greater significant differences were noted in adolescents with obesity and metabolic syndrome, especially in large and small subclasses, and VLDL diameter seemed to be useful to differentiate levels of cardiac involvement. The hypersecretion of large VLDL-P, as a result of overnutrition and insulin resistance, has been previously proposed as a key pathological mechanism in atherogenic dyslipidemia.[34,35]

Cardioprotective functions of HDL include, in addition to the reverse cholesterol transport to the liver, the inhibition of LDL oxidation and anti-inflammatory actions in the endothelium.[36,37] However, in conditions of hypertriglyceridemia and insulin resistance, the overstimulated cholesteryl-ester-transfer protein enriches HDL composition in TG by means of exchanging TG by cholesteryl esters with other lipoprotein subclasses.[38-40] Consequently, TG-enriched HDL have their beneficial features reduced – in T2-DM patients by up to 52% of the HDL antioxidative capacity[41] – and have been associated with atheroma plaque formation.[42] Our results have highlighted the prevalence of TG-enriched HDL among participants with cardiac changes and especially in those with MS, as well as a relationship between TG-enriched HDL and LDL and the insulin resistance. Hence, the HDL's cardioprotective function might be decreased in these subjects.

Furthermore, a reduced number of total and medium HDL-P concentration and size has been associated with higher CVD risk in adults,[43,44] and previous studies conducted in obese adolescents with insulin resistance or T2-DM noted a significant decrease in large HDL-P.[45] Nevertheless, these findings were not reproduced in the descriptive analysis of our cohort, where the significant reduction was shown in the total HDL-P concentration, without significant distinctions between the subclasses, however the large HDL-P reduction was identified as a differentiating factor between mild and severe cardiac changes in the multivariable analysis, which gives prominence to the widely recognized role of smaller diameter HDL in CVD.[46]

Remnant cholesterol marks the overall load of TG-rich lipoproteins (VLDL and IDL), which in situations of hypertriglyceridemia can carry as much or more cholesterol than LDL.[47] How it interacts in the atherosclerosis physiopathology is still unclear but its association with CVD, as a factor related to coronary artery disease, has been established and an increased risk – up to 2.7 times in concentrations ≥39 mg/dL – has been reported as independent of obesity.[4] The highest remnant cholesterol values in the present study were near to this hypothetical threshold and belonged to obese adolescents with metabolic syndrome, who also were the subjects with the highest triglycerid levels. However, a close relationship with cardiac changes was not demonstrated.

This study has some limitations. The cross-sectional design and small sample size limit the extraction of causal conclusions. The criteria for the degrees of cardiac involvement have been defined by the authors and have not been previously tested in other publications. They are based on the concept that severity increases with the

addition of cardiac changes, from only LV remodeling to systolic dysfunction in the obese subjects, defined by GLS, a widely studied parameter linked to mortality.[48] The diastolic function was not included in the group definition criteria because of the lack of a single parameter for its identification, but the early GLSR was incorporated to the correlation analysis instead.

6.5 Conclusions

In conclusion, our results have shown that morbidly obese adolescents present an atherosclerotic ALT despite showing no pathological concentrations in the conventional lipid profile. Furthermore, when these obese adolescents are classified by the degree of cardiac change, ALT and GlycA appear to provide more reliable indicators of severity than traditional CV risk factors as BMI, BP or insulin resistance.

6.6 Tables and Figures

Table 1: Clinical and laboratory characteristics of subjects depending on cardiac involvement degree groups.

Variable	No cardiac disorder (N=25)	Mild cardiac changes (N=17)	Severe cardiac changes (N=25)	P value		
				No vs Mild	No vs Severe	Mild vs Severe
Age (years)	14 [13-15]	14 [13-16]	14 [13-15]	0.17	0.74	0.23
BMI (kg/m²)	19.5 [17.9-22.7]	35.2 [32.7-38.9]	37.8 [34.9-40.2]	**<0.01**	**<0.01**	0.15
BMI SD	-0.1 [-0.9-1.1]	7.0 [5.9-8.4]	7.8 [6.4-9.0]	**<0.01**	**<0.01**	0.26
SBP (mmHg)	113 [101-119]	120 [114-128]	126 [119-141]	**<0.01**	**<0.01**	0.08
DBP (mmHg)	64 [57-69]	66 [59-76]	76 [67-81]	0.35	**<0.01**	0.05
BP ≥p90 (%)	12	35	68	0.12	**<0.01**	0.05
LABORATORY PARAMETERS						
Fasting glucose (mg/dL)	79 [71-84]	82 [72-90]	83 [78-88]	0.27	**0.02**	0.66
HbA1c (%) (N=57)	5.2 [5.1-5.5]	5.3 [5.2-5.5]	5.4 [5.2-5.6]	0.29	0.17	0.65
HOMA-IR	1.4 [1.0-2.3]	3.6 [1.8-5.0]	6.6 [3.8-8.2]	**<0.01**	**<0.01**	**<0.01**
Classical lipid profile						
Total Cholesterol (mg/dL)	173 [164-188]	181 [143-201]	179 [169-198]	0.74	0.28	0.72
LDL-C (mg/dL)	103 [91-113]	98 [77-120]	106 [96-121]	0.63	0.32	0.25
HDL-C (mg/dL)	52 [45-60]	44 [41-55]	44 [41-48]	0.07	**<0.01**	0.37
Triglycerides (mg/dL)	71 [60-92]	95 [75-118]	87 [74-140]	**0.02**	**0.01**	0.92
Remnant cholesterol (mg/dL)	18.9 [13.5-22.5]	24.2 [17.5-30.3]	22.0 [18.1-36.9]	**0.03**	**0.01**	0.99
HDL-C ≤40 mg/dL (%)	0	18	14	0.05	0.23	0.67
Triglycerides ≥150 mg/dL (%)	0	12	16	0.15	0.11	1

Inflammatory markers						
Highly sensitive C-reactive protein (mg/dL) (N=63)	0.02 [0.01-0.09]	0.12 [0.06-0.24]	0.24 [0.14-0.52]	**<0.01**	**<0.01**	**0.03**
Glycoprotein A (µmol/L)	618 [583-747]	707 [659-830]	845 [731-982]	**<0.01**	**<0.01**	**0.01**
LIPOPROTEIN PARTICLES						
VLDL-P (nmol/L)						
Total	30.1 [25.5-40.7]	45.0 [29.3-55.1]	37.4 [31.6-69.5]	**0.04**	**<0.01**	0.72
Large	0.8 [0.7-1.2]	1.3 [0.9-1.6]	1.1 [0.9-1.6]	**0.03**	**<0.01**	0.92
Medium	3.3 [2.6-5.0]	4.7 [3.6-8.0]	5.0 [2.7-6.2]	**0.02**	0.11	0.63
Small	26.1 [22.7-33.6]	39.3 [25.0-47.3]	30.1 [27.6-59.9]	0.06	**<0.01**	0.67
LDL-P (nmol/L)						
Total	1023.6 [913.5-1131.3]	1017.8 [818.1-1182.7]	1123.0 [1015.8-1245.2]	0.86	**0.03**	0.11
Large	165.0 [151.6-174.9]	163.8 [129.8-188.7]	172.3 [147.3-183.0]	0.58	0.72	0.49
Medium	300.4 [248.3-356.3]	299.0 [146.3-378.2]	335.7 [257.6-381.7]	0.63	0.29	0.24
Small	560.0 [517.1-599.2]	565.0 [522.8-639.0]	625.1 [551.7-685.3]	0.40	**<0.01**	0.07
HDL-P (µmol/L)						
Total	26.5 [23.7-29.3]	24.3 [20.6-29.0]	24.2 [22.1-25.6]	0.24	**0.01**	0.54
Large	0.22 [0.2-0.3]	0.26 [0.2-0.3]	0.25 [0.2-0.3]	**<0.01**	**0.03**	0.14
Medium	9.3 [8.6-10.4]	9.0 [8.1-10.3]	8.9 [7.9-9.3]	0.36	**0.03**	0.39
Small	16.8 [14.5-18.9]	15.2 [12.0-19.2]	14.8 [13.2-16.4]	0.40	**0.02**	0.59
Size (nm)						
VLDL size	42.3 [42.0-42.4]	42.4 [42.3-42.4]	42.1 [42.0-42.3]	0.33	0.21	**0.03**
LDL size	21.1 [20.9-21.2]	21.0 [20.7-21.2]	21.0 [20.9-21.1]	0.06	**0.04**	0.63
HDL size	8.3 [8.2-8.3]	8.3 [8.2-8.4]	8.3 [8.2-8.3]	0.43	0.23	0.99
Composition						
Ratio VLDL-TG/VLDL-C	3.70 [3.4-4.0]	3.62 [3.5-4.1]	3.9 [3.5-4.2]	0.92	0.36	0.51
Ratio IDL-TG/IDL-C	1.20 [1.1-1.4]	1.20 [1.1-1.4]	1.10 [1.1-1.2]	0.86	0.14	0.16
Ratio LDL-TG/LDL-C	0.11 [0.1-0.1]	0.12 [0.1-0.1]	0.14 [0.1-0.2]	0.82	**<0.01**	0.07
Ratio HDL-TG/HDL-C	0.23 [0.2-0.3]	0.29 [0.2-0.4]	0.30 [0.2-0.4]	**0.01**	**<0.01**	0.90
Ratio LDL-P/HDL-P	40.0 [31.7-47.6]	43.9 [34.4-45.9]	47.1 [40.7-53.1]	0.65	**<0.01**	**0.03**
Non-HDL-P (nmol/L)	1034.7 [934.9-1148.1]	1122.0 [837.8-1228.5]	1153.1 [1042.3-1282.1]	0.92	**0.01**	0.14

Values expressed in median and 25-75% IQR; P value calculated by non-parametric Mann-Whitney U test; Dichotomous variables (Fisher exact test); BMI, Body Mass Index; SD, Standard deviation; SBP, Systolic blood pressure; DBP, Diastolic blood pressure; HOMA-IR, Homeostatic model assessment insulin resistance.

Table 2: Clinical and laboratory characteristics of subjects depending on body mass index groups.

Variable	Non-obese (N = 25)	Obese (N = 42)	P value
Age (years)	14 [13-15]	14 [13-15]	0.72
Male	52 %	33 %	0.19
BMI (kg/m^2)	19.4 [17.9-22.1]	36.8 [34.3-39.8]	**<0.01**
BMI SD	-0.2 [-0.9-0.7]	7.5 [6.4-8.5]	**<0.01**
Waist circumference (cm)	69 [65-74]	111 [102-120]	**<0.01**
SBP (mmHg)	108 [101-118]	124 [118-134]	**<0.01**
DBP (mmHg)	60 [60-68]	74 [65-78]	**<0.01**
LABORATORY PARAMETERS			
Fasting glucose (mg/dL)	76 [71-84]	83 [75-89]	**0.01**
HbA1c (%) (N=57)	5.2 [5.1-5.5]	5.3 [5.2-5.5]	0.21
HOMA-IR	1.2 [1.0-1.7]	5 [3.6-7.9]	**<0.01**
Classical lipid profile			
Total Cholesterol (mg/dL)	180 [164-191]	178 [156-197]	0.61
LDL-C (mg/dL)	102 [90-115]	105 [91-118]	0.60
HDL-C (mg/dL)	52 [48-61]	44 [41-49]	**<0.01**
Triglycerides (mg/dL)	77 [60-90]	91 [72-130]	**<0.01**
Remnant cholesterol (mg/dL)	19.1 [14.1-22.5]	23.9 [18.0-36.3]	**0.01**
Inflammatory markers			
Highly-sensitive C-reactive protein (mg/dL)	0.02 [0.01-0.05]	0.22 [0.13-0.45]	**<0.01**
Glycoprotein A (µmol/L)	620 [583-687]	802 [705-938]	**<0.01**
LIPOPROTEIN PARTICLES			
VLDL-P (nmol/L)			
Total	30.0 [25.5-40.7]	42.8 [31.5-63.7]	**<0.01**
Large	0.8 [0.7-1.2]	1.3 [0.9-1.6]	**<0.01**
Medium	3.7 [2.8-5.4]	4.6 [3.0-6.5]	0.07
Small	26.1 [22.4-33.6]	37.3 [27.3-55.6]	**<0.01**
LDL-P (nmol/L)			
Total	1023.6 [904.7-1136.9]	1096.5 [977.4-1196.7]	0.13
Large	165.1 [150.6-183.3]	164.4 [145.2-182.5]	0.72
Medium	300.4 [225.2-356.3]	332.1 [249.9-384.6]	0.37
Small	560.0 [517.1-607.0]	616.2 [527.3-676.3]	**0.01**
HDL-P (µmol/L)			

Total	27.0 [24.2-30.1]	24.2 [21.7-26.4]	**<0.01**
Large	0.2 [0.2-0.3]	0.2 [0.2-0.3]	**0.01**
Medium	9.6 [8.7-10.9]	8.9 [7.9-9.4]	**0.01**
Small	17.3 [14.8-19.2]	17.8 [12.8-17.0]	**<0.01**
Size (nm)			
VLDL size	42.3 [42.2-42.4]	42.2 [42.0-42.4]	0.37
LDL size	21.1 [21.0-21.2]	21.0 [20.9-21.1]	0.05
HDL size	8.3 [8.2-8.3]	8.3 [8.2-8.3]	0.12
Composition			
Ratio VLDL-TG/VLDL-C	3.7 [3.4-3.9]	3.9 [3.5-4.2]	0.24
Ratio IDL-TG/IDL-C	1.2 [1.1-1.4]	1.1 [1.1-1.3]	**0.04**
Ratio LDL-TG/LDL-C	0.1 [0.1-0.1]	0.1 [0.1-0.2]	**0.02**
Ratio HDL-TG/HDL-C	0.2 [0.2-0.3]	0.3 [0.2-0.4]	**<0.01**
Ratio LDL-P/HDL-P	37.1 [31.7-45.2]	46.2 [38.9-51.8]	**<0.01**
Non-HDL-P (nmol/L)	1034.7 [915.5-1163.1]	1127.8 [1002.7-1245.4]	0.06

Values expressed in median and 25-75% IQR; P value calculated by non-parametric Mann-Whitney U test; Dichotomous variables (Fisher exact test); BMI, Body Mass Index; SD, Standard deviation; SBP, Systolic blood pressure; DBP, Diastolic blood pressure; HOMA-IR, Homeostatic model assessment insulin resistance.

Table 3: Clinical and laboratory characteristics of subjects depending on metabolic syndrome (MS) diagnosis.

Variable	No MS (<3 factors) (N=53)	MS (≥3 factors) (N=14)	P value
Age (years)	14 [13-15]	14 [13-15]	0.82
BMI (kg/m^2)	32.1 [19.4-37.0]	38.1 [35.9-43.0]	**<0.01**
BMI SD	5.7 [-0.1-7.5]	7.9 [6.5-10.3]	**<0.01**
SBP (mmHg)	118 [106-122]	131 [126-144]	**<0.01**
DBP (mmHg)	67 [59-74]	77 [69-80]	**<0.01**
LABORATORY PARAMETERS			
Fasting glucose (mg/dL)	79 [72-86]	84 [82-89]	**0.02**
HbA1c (%) (N=57)	5.3 [5.1-5.5]	5.4 [5.1-5.6]	0.51
HOMA-IR	2.3 [1.3-4.7]	7.4 [4.2-8.9]	**<0.01**
Classical lipid profile			
Total Cholesterol (mg/dL)	176 [164-193]	188 [164-207]	0.18
LDL-C (mg/dL)	103 [90-117]	105 [95-121]	0.63
HDL-C (mg/dL)	49 [43-56]	42 [36-47]	**<0.01**
Triglycerides (mg/dL)	78 [64-99]	124 [103-163]	**<0.01**
Remnant cholesterol (mg/dL)	19.6 [14.6-24.1]	30.3 [25.2-44.4]	**<0.01**
Inflammatory markers			
Highly sensitive C-reactive protein (mg/dL)	0.09 [0.02-0.21]	0.37 [0.15-0.50]	**<0.01**
Glycoprotein A (µmol/L)	701 [616-787]	868 [777-999]	**<0.01**
LIPOPROTEIN PARTICLES			
VLDL-P (nmol/L)			
Total	31.7 [26.9-45.0]	59.6 [47.6-82.5]	**<0.01**
Large	0.9 [0.7-1.3]	1.6 [1.3-1.8]	**<0.01**
Medium	3.7 [2.6-5.4]	6.1 [4.5-9.4]	**<0.01**
Small	28.3 [23.3-38.6]	52.2 [40.1-71.4]	**<0.01**

LDL-P (nmol/L)			
Total	1033.2 [913.5-1175.2]	1092.5 [998.0-1256.9]	0.23
Large	165.1 [146.0-183.3]	161.1 [147.8-180.5]	0.84
Medium	311.5 [232.6-368.0]	347.7 [256.5-377.1]	0.60
Small	575.8 [529.4-627.0]	644.2 [518.6-714.6]	0.11
HDL-P (µmol/L)			
Total	25.5 [23.0-28.7]	23.5 [20.3-26.0]	0.09
Large	0.2 [0.2-0.3]	0.3 [0.2-0.3]	0.15
Medium	9.1 [8.4-9.9]	8.3 [7.5-9.5]	0.07
Small	16.2 [13.9-18.7]	14.6 [12.3-16.5]	0.09
Size (nm)			
VLDL size	42.3 [42.0-42.4]	42.2 [42.1-42.4]	0.87
LDL size	21.0 [20.9-21.2]	20.9 [20.8-21.0]	0.11
HDL size	8.3 [8.2-8.3]	8.3 [8.3-8.3]	0.31
Composition			
Ratio VLDL-TG/VLDL-C	3.7 [3.5-4.1]	4.0 [3.5-4.2]	0.26
Ratio IDL-TG/IDL-C	1.2 [1.1-1.4]	1.1 [1.1-1.2]	0.06
Ratio LDL-TG/LDL-C	0.1 [0.1-0.1]	0.1 [0.1-0.2]	**<0.01**
Ratio HDL-TG/HDL-C	0.2 [0.2-0.3]	0.4 [0.3-0.5]	**<0.01**
Ratio LDL-P/HDL-P	42.1 [33.6-47.3]	49.5 [43.3-52.8]	**<0.01**
Non-HDL-P (nmol/L)	1066.3 [934.9-1194.3]	1127.8 [1027.1-1317.5]	0.08

Values expressed in median and 25-75% IQR; P value calculated by non-parametric Mann-Whitney U test; Dichotomous variables (Fisher exact test); BMI, Body Mass Index; SD, Standard deviation; SBP, Systolic blood pressure; DBP, Diastolic blood pressure; HOMA-IR, Homeostatic model assessment insulin resistance.

Table 4: Bivariate Correlations between lipoprotein particles and left ventricle structural and functional parameters, insulin resistance index, inflammatory marker and triglycerides.

	Remodeling	Systolic GLS	Early GLSR	HOMA	hs-CPR	TG
VLDL-P (nmol/L)						
Total	0.37*	0.30†	-0.28†	0.52*	0.23	0.96*
Large	0.39*	0.32*	-0.31*	0.53*	0.25†	0.91*
Medium	0.30†	0.12	-0.12	0.35†	0.08	0.91*
Small	0.38*	0.33*	-0.30†	0.53*	0.25†	0.95*
LDL-P (nmol/L)						
Total	0.18	0.16	-0.11	0.28†	0.21	0.33*
Large	-0.05	-0.08	0.13	0.06	-0.04	0.28†
Medium	0.07	0.05	-0.03	0.22	0.14	0.35*
Small	0.30†	0.32*	-0.25†	0.30†	0.34*	0.21
HDL-P (µmol/L)						
Total	-0.24†	-0.42*	0.44*	-0.33*	-0.51*	0.14
Large	0.40*	0.11	-0.23	0.25†	0.17	0.49*
Medium	-0.19	-0.36*	0.39*	-0.23	-0.39*	0.06
Small	-0.20	-0.36*	0.37*	-0.30†	-0.47*	0.13
Size (nm)						
VLDL size	0.06	-0.19	0.16	-0.09	-0.21	0.29†
LDL size	-0.25†	-0.25†	0.23	-0.07	-0.25†	0.17
HDL size	0.13	0.15	-0.17	0.15	0.27†	-0.09
Composition						
Ratio VLDL-TG/VLDL-C	0.05	0.19	-0.04	0.14	0.25†	-0.04
Ratio IDL-TG/IDL-C	-0.16	-0.20	0.22	-0.36*	-0.32*	0.45*

Ratio LDL-TG/LDL-C	0.29†	0.29†	-0.25†	0.47*	0.30†	0.65*
Ratio HDL-TG/HDL-C	0.40*	0.30†	-0.33*	0.52*	0.33*	0.88*
Ratio LDL-P/HDL-P	0.27†	0.42*	-0.37*	0.45*	0.51*	0.18
Non-HDL-P (nmol/L)	0.23	0.20	-0.15	0.33†	0.24	0.42*
Remnant cholesterol (mg/dL)	0.35*	0.23	-0.25†	0.46†	0.20	0.97*

Spearman coefficient. Values expressed in r. *p<0.01. †p<0.05. GLS, Global longitudinal strain; GLSR, Global longitudinal strain rate; HOMA-IR, Homeostatic model assessment insulin resistance; hs-CRP, highly-sensitive C-reactive protein; TG, triglycerides.

Table S1: Echocardiographic data of cardiac involvement groups

Variable	No cardiac disorder (N=25)	Mild cardiac changes (N=17)	Severe cardiac changes (N=25)	P value		
				No vs Mild	No vs Severe	Mild vs Severe
LV mass index (g/ht$^{2.7}$)	30.7 [26.6-35.7]	46.3 [39.4-57.4]	48.1 [44.4-54.6]	**<0.01**	**<0.01**	0.43
RWT	0.32 [0.30-0.36]	0.40 [0.34-0.45]	0.40 [0.35-0.43]	**<0.01**	**<0.01**	0.72
LV remodeling (%)	0	88	100	**<0.01**	**<0.01**	0.15
Systolic GLS (%)	-20.9 [-23.1 to -18.9]	-17.5 [-18.7 to -17.0]	-14.4 [-16.1 to -13.4]	**<0.01**	**<0.01**	**<0.01**
Early diastolic GLSR (1/s)	3.1 [2.8-3.3]	2.3 [2.1-2.6]	2.0 [1.8-2.2]	**<0.01**	**<0.01**	**0.01**

Values expressed in median and 25-75% IQR; P value calculated by non-parametric Mann-Whitney U test; Dichotomous variables (Fisher exact test); LV, Left ventricle; RWT, Relative wall thickness; GLS, Global longitudinal strain; GLSR, Global longitudinal strain rate.

Table S2: Bivariate Correlations between lipoprotein particles and components of conventional lipid profile.

	Total Cholesterol	LDL-C	HDL-C	TG	Remnant cholesterol
VLDL-P (nmol/L)					
Total	0.43*	0.16	-0.29†	0.96*	0.95*
Large	0.36*	0.11	-0.33*	0.91*	0.90*
Medium	0.40*	0.12	-0.18	0.91*	0.89*
Small	0.42*	0.15	-0.29†	0.95*	0.94*
LDL-P (nmol/L)					
Total	0.87*	0.96*	0.02	0.33*	0.36*
Large	0.83*	0.87*	0.17	0.28†	0.33*
Medium	0.83*	0.89*	0.06	0.35*	0.37*
Small	0.61*	0.71*	-0.09	0.21	0.21
HDL-P (µmol/L)					
Total	0.36*	0.02	0.86*	0.14	0.11
Large	0.49*	0.19	0.04	0.49*	0.48*
Medium	0.32*	-0.03	0.70*	0.06	0.03
Small	0.31*	0.05	0.75*	0.13	0.11
Size (nm)					
VLDL size	0.05	-0.07	0.04	0.29†	0.29†
LDL size	0.41*	0.39*	0.25†	0.17	0.21
HDL size	-0.06	-0.04	-0.31*	-0.09	-0.06
Composition					
Ratio VLDL-TG/VLDL-C	-0.13	0.36	-0.13	-0.04	-0.19
Ratio IDL-TG/IDL-C	-0.54*	-0.48*	0.17	0.45*	-0.51*
Ratio LDL-TG/LDL-C	0.40*	0.21	-0.18	0.65*	0.64*
Ratio HDL-TG/HDL-C	0.23	-0.03	-0.37*	0.88*	0.85*
Ratio LDL-P/HDL-P	0.37*	0.66*	-0.57*	0.18	0.22
Non-HDL-P (nmol/L)	0.89*	0.93*	-0.01	0.42*	0.44*

Spearman coefficient. Values expressed in r. *p<0.01. †p<0.05. LDL, Low-density Lipoprotein; HDL, High-density Lipoprotein; TG, triglycerides.

Figure 1: The lipid contour is a graphical model to facilitate the lipoprotein profile interpretation and its association with cardiovascular risk. The colored silhouettes represent the patient groups' values with respect to the values of an apparently healthy population (black circle).[49] The study group's contour delimits a smaller central area when the variables have values associated with an increased risk of developing CVD (i.e., values higher than the reference population's mean for L-VLDL-P, VLDL-P, Rem-C, S-LDL-P, LDL-P, HDL-TG/HDL-C variables; or lower than reference population's mean for LDL-Ø, HDL-P and M-HDL-P variables). Colored silhouettes are represented in percentage of increase or reduction regarding data in tables 1-3.

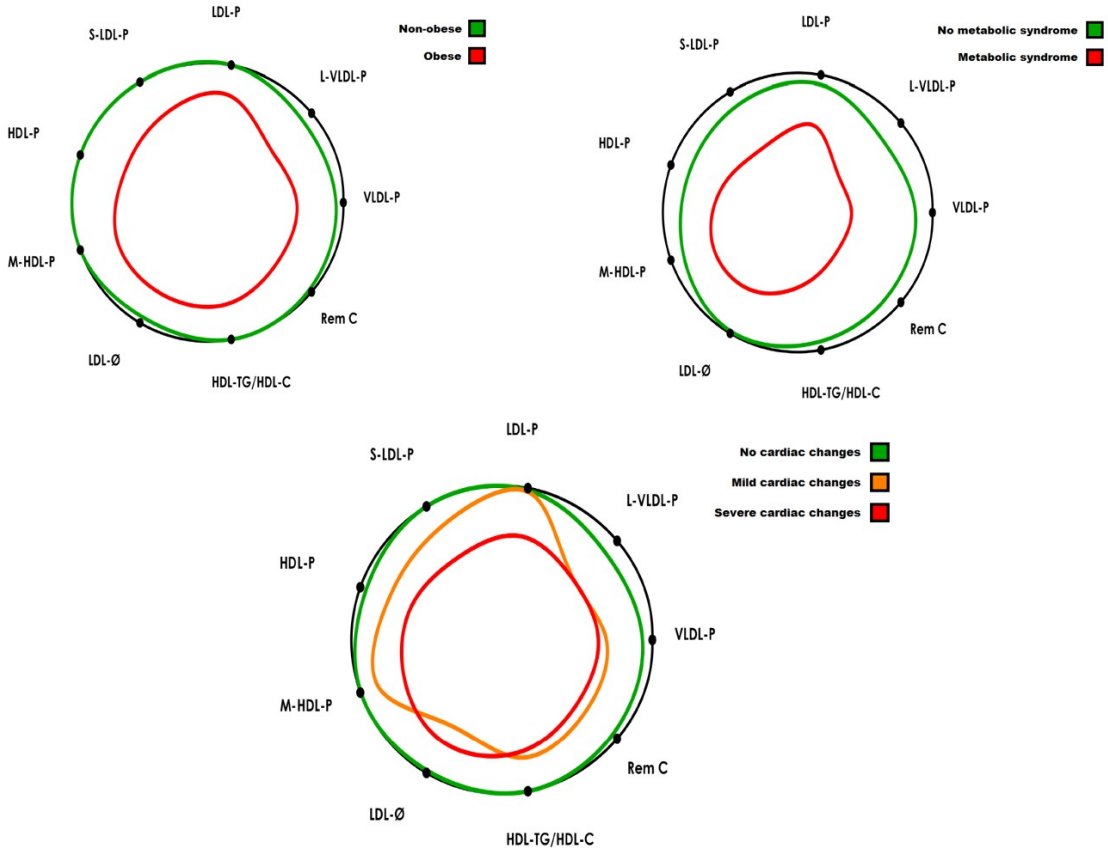

VLDL-P, total VLDL particles; L-VLDL-P, large VLDL particles; LDL-P, total LDL particles; S-LDL-P, small LDL particles; HDL-P, total HDL particles; M-HDL-P, medium HDL particles; LDL-Ø, LDL particles diameter; HDL-TG/HDL-C, triglyceride enriched HDL; Rem C, remnant cholesterol.

Figure 2: Multivariable model to differentiate mild cardiac change subjects (1) than those with severe cardiac changes (2). The variables included in the model were those that overlap by at least two of the three statistical approaches. An area under the curve (AUC) of 0.79 (95% CI: 0.54-1) was obtained with the next pattern: HOMA-IR, glycoprotein A (Glyc-A), VLDL diameter and large HDL-P. Predictive accuracy = 0.8; p-value = 0.051; out-of-bag error = 0.27.

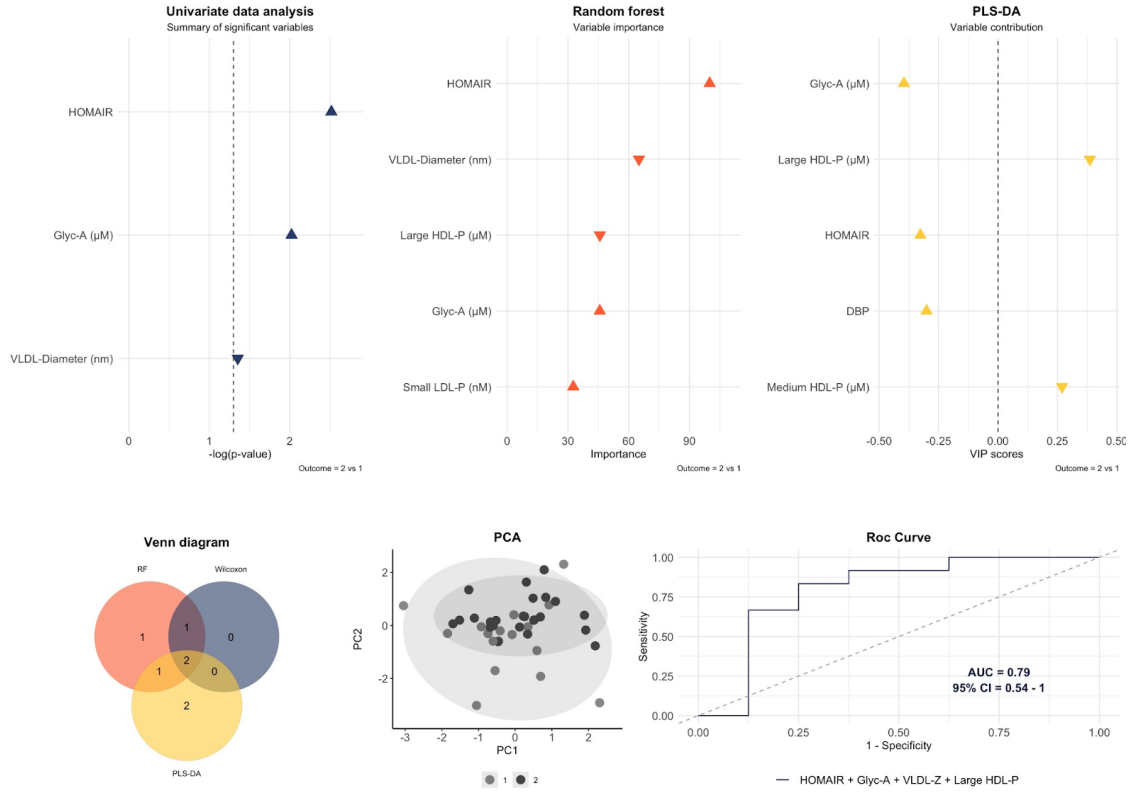

Figure 3: Multivariable model to differentiate normal heart subjects (0) from those with severe cardiac changes (2). The variables included in the model were those that overlap by the three statistical approaches. An area under the curve (AUC) of 0.91 (95% CI: 0.74-1) was obtained with the next pattern: body mass index standard deviation (BMIsd), HOMA-IR, systolic blood pressure (SBP), diastolic blood pressure (DBP), glycoprotein A (Glyc-A), small VLDL-P, small LDL-P and ratio HDL-TG/HDL-C. Predictive accuracy = 0.84; p-value = 0.004; out-of-bag error = 0.1.

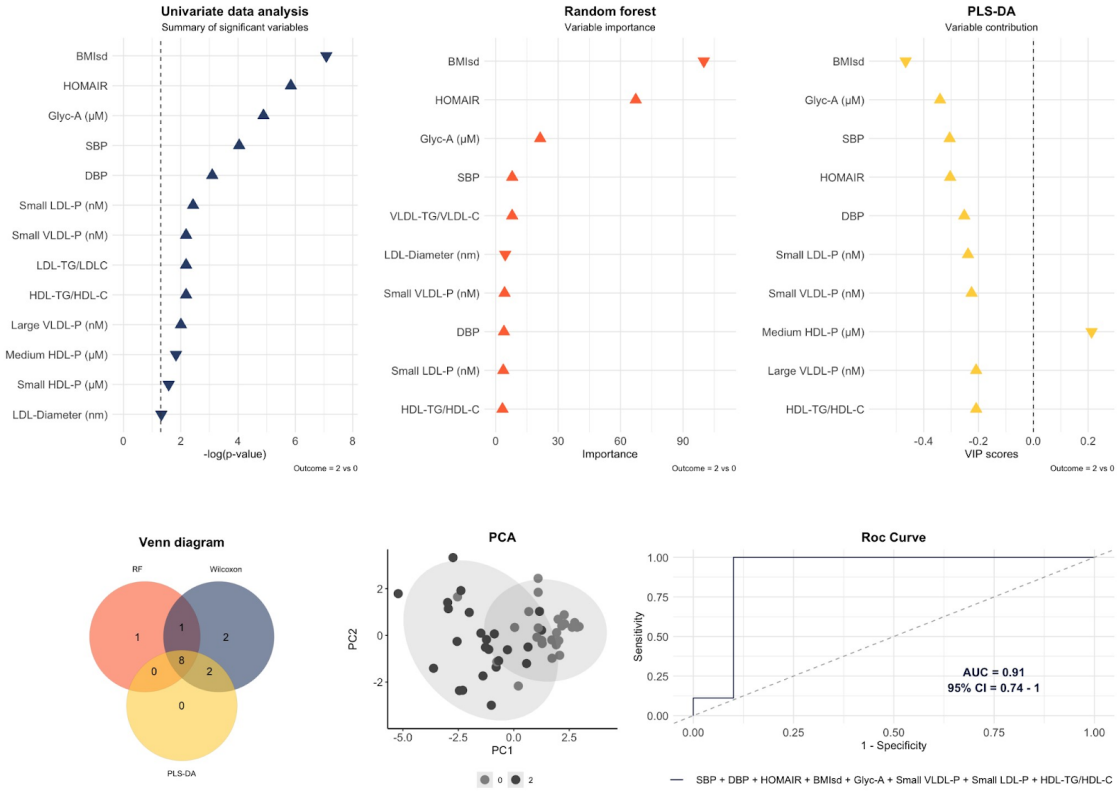

Figure 4: Comparative analysis between ROC curves considering only traditional cardiovascular risk factors (body mass index standard deviation, blood pressure and HOMA-IR) and ROC curves shown in Figure 2 and 3. A) When normal heart subjects were compared to those with severe cardiac changes, the addition of lipoprotein subclasses and glycoprotein A to the model with traditional risk factors did not change the area under the curve (AUC) (0.92 vs 0.91) [Only traditional risk factors: AUC 0.92 (95% CI: 0.77-1); predictive accuracy = 0.88; p-value = 0.0001; out-of-bag error = 0.1]. B) When mild cardiac change subjects were compared to those with severe cardiac changes, the addition of lipoprotein subclasses and glycoprotein A caused an increase in the AUC (0.58 vs 0.79) [Only traditional risk factors: AUC 0.58 (95% CI: 0.3-0.86); predictive accuracy = 0.6; p-value = 0.596; out-of-bag error = 0.32].

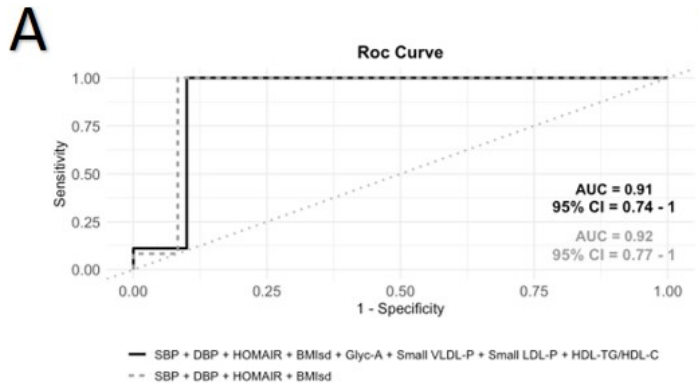

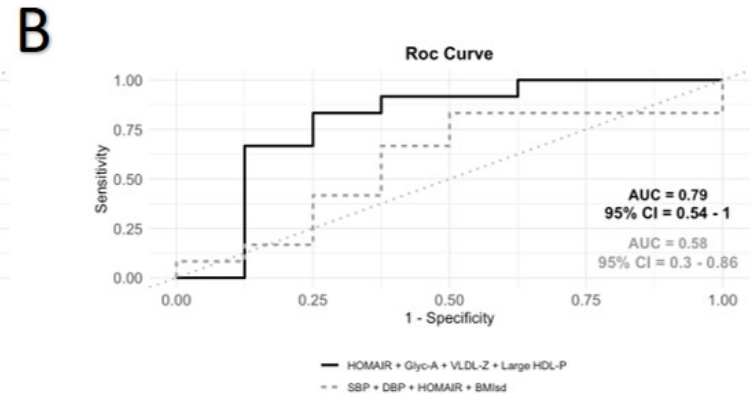

7. MYOCARDIAL TISSUE CHARACTERIZATION AND PERICARDIAL FAT STUDY

7.1 Introduction

Obesity and some of its comorbidities are pathologies with a high risk of developing secondary cardiomyopathies because of their capacity for triggering changes in the myocardium interstitium –characterized by myofibroblast development, inflammation and disrupted formation of metalloproteinases– and leading to modifications of the extracellular matrix (ECM) as well as intrinsic myocardium deteriorations.[1] This cardiomyopathy final stage is characterized by a diffuse myocardial fibrosis, which, unlike with post-infarction cardiomyopathy, possesses a prolonged subclinical course before the onset of symptoms.[2]

T1 mapping is a cardiovascular magnetic resonance (CMR) technique that quantifies changes to the ECM, disrupted as a result of diffuse reactive fibrosis or substance deposits.[3-5] T1 mapping has demonstrated its value in assessing myocardial changes in pathologies that involve interstitial fibrosis.[6,7] Conversely, when cardiovascular risk factors induce myocardial changes but no underlying cardiomyopathy, the native T1 time has been unaffected.[8] Moreover, due to its capacity

for assessing myocardium inflammation and fibrosis, native T1 could be a useful technique for evaluating the impact of obesity's low-grade inflammation in the myocardium and detecting the obese patients at higher risk of developing a non-ischemic cardiomiopathy.[9,10] However, to our knowledge, the few studies conducted in obese adults have generated opposite conclusions and the obese pediatric population has not been previously evaluated.[11,12]

The adipose tissue around the heart has the ability of affecting the myocardium by the release of pro-inflammatory molecules such as cytokines and adipokines. The pericardial fat, defined as the sum of the epicardial fat and the paracardial fat, has previously been related in children with cardiovascular risk factors and cardiac changes[13] however, no study has assessed its relationship with T1 mapping.

The present has the objectives of quantifying the native T1 and T2 times and the pericardial fat volume, and determining their relationship with LV morphology, cardiovascular risk factors, inflammatory parameters and hepatic steatosis.

7.2 Methodology

7.2.1 Study Population

We studied 38 adolescents of both genders between 10 and 17 years old. Subjects with obesity were recruited from endocrinology clinics of participating hospitals and control participants were recruited from healthy volunteers in the cardiology and sports medicine clinics. Two groups were identified: the study group with morbid obesity (SDS-BMI ≥4; n = 25), and the control subjects (BMI 5th-85th

percentile, n = 13) according to tables from the Barcelona Longitudinal Growth Study 1995–2017.[14] The control group adolescents were paired by age and gender, with a ratio of 2 cases: 1 control, for minimizing the confounding effects.

Subjects with current infections or recent acute inflammatory processes, a history of prematurity or birth weight <2000 g, and smokers or those with pathologies that could change the arterial or myocardial wall – such as congenital heart disease, chronic kidney disease, transplants, rheumatic disease, infection by HIV virus – were excluded. Similarly, subjects with type 2 DM (T2-DM) were excluded. Preventive measures taken to avoid potential confounding variables in subjects recruited in the sports clinic are explained in a previous study.[15]

Written informed consent for participation was obtained and the Institutional Review Board at Vall d'Hebron Hospital approved the protocol (PR-AMI-273/2018). All subjects provided assent and an informed consent was signed by their parents/legal guardians.

7.2.2 Clinical and Laboratory Assessment

Demographic data of age, gender and clinical status were obtained from patient anamnesis. Systolic and diastolic blood pressures (SBP and DBP) were obtained using a Welch Allyn Spot Vital Signs Monitor (4200B, Hillrom, Batesville, Indiana) after subjects had rested for 5 minutes, in a supine position and with an appropriately sized cuff giving measured mid-arm circumference, according to the criteria of the European Society of Hypertension,[16] which defines also the high BP values by age and gender.

EDTA blood samples were obtained at the time of enrollment at the participating hospitals in the morning after at least 8 hours of fasting. Samples for lipoprotein particle analysis were aliquoted, stored in liquid nitrogen (−80° C) and dispatched on dry ice to Biosfer Teslab, where lipoprotein particle concentrations were measured by proton nuclear magnetic resonance spectroscopy, based on the LipoScale test®.[17] Tests performed on blood samples in all subjects were: white blood cell count, pro-inflammatory molecules (highly sensitive C-reactive protein [hs-CRP] and interleukin 6), fasting glycemia and insulin, glycated hemoglobin, total cholesterol, high-density lipoprotein (HDL), low-density lipoprotein (LDL) and triglycerides (TG). To evaluate insulin resistance, the homeostasis model assessment of insulin resistance (HOMA-IR) was calculated using the equation: fasting insulin (µU/ml) × fasting glucose (mmol/l) / 22.5.

7.2.3 CMR Image Acquisition

CMR was performed with a 1.5 Tesla MR System Avanto-fit syngo MRE11 (Siemens Healthcare, Erlangen, Germany), by using a 32-channel torso phased-array coil. Cine images were obtained in three long-axis views, and in the short-axis plane covering the heart's base to apex. LV tissue characterization included T2-weighted image, and end-diastolic T1 and T2 mapping.

Native T1 mapping was performed using an electrocardiogram-triggered Modified Look-Locker Inversion recovery (MOLLI) sequence and quantitative values were acquired placing regions of interest (ROI) in the interventricular septum and LV posterior wall at basal, mid-ventricular and apical LV myocardium in the short-axis

plane. Imaging parameters were adapted from previously published studies: temporal resolution of 15 sec, echo time of 1.11 msec, inversion time 180 msec, field of view of 360 x 307 mm, and voxel size of 1.9 x 1.9 x 6 mm.

Analysis was performed offline on dedicated software (IntelliSpace Portal, version 10.1; Philips Medical Systems). The images were evaluated independently by two experienced radiologists (L.R. and Ll.R.). The endocardium and epicardium were contoured in the short-axis plane to calculate the LV end-diastolic and end-systolic volumes, LV mass index (LVMI) and LV ejection fraction. These parameters were indexed to the body surface area.[18] The global native T1 value (native T1) and T2 values were calculated as the average of all measurements in the short-axis plane.[19,20] Additionally, the native T1 values in LV septum (native-T1s) and posterior wall (native-T1pw) were estimated as the measurements' average in each ROI.

7.2.4 Pericardial Fat Index

The pericardial adipose volume was obtained by 1.5 Tesla MR System Avanto-fit syngo MRE11 (Siemens Healthcare, Erlangen, Germany). Twenty-five axial sections SSFP cine stack of the heart were obtained with contiguous 4 mm slice thickness and 10 mm interslice gap.

Off-line image analysis for pericardial fat on the axial SSFP cine stack was performed by Tumor Tracking software of the Argus analysis program (Siemens Medical Systems, Erlangen, Germany). The fat tissue included was that confined between the chest wall and the myocardium, and between the last slice where the ventricle was visible and the plane of pulmonary artery bifurcation. Measurements were manually

performed by a single trained observer blinded to the patient data. The pericardial fat index (PFI) was the result of: pericardial fat volume x 0.916 g/mL (fat density) / height in meters to the power of 3.[21]

7.2.5 Hepatic Fat Fraction

The hepatic fat fraction (HFF) was obtained with 1.5 Tesla MR System Avanto-fit syngo MR E11 (Siemens Healthcare, Erlangen, Germany) by using a two-dimensional spoiled GRE sequence. To reduce T1 contrast, a flip angle of 20° was used with a repetition time of 120 msec. To estimate MR imaging HFF, a single gradient echo sequence with 8-10 echoes was acquired at serial opposed-phase and in-phase echo times (1.2, 2.4, 3.6, 4.8, 6.0 and 7.2 msec) during a single breath hold of 15 seconds. Other imaging parameters were 7-8 mm section thickness, 10 mm interslice gap, bandwidth adapted to echo time multiple of 1.2, one excitation acquired, and a field of view of 40 cm with a 128 × 116 matrix.

7.2.6 Reproducibility

Variability in the measurement of pericardial fat volume, made by a single cardiologist, was evaluated in 10 randomly selected individuals by different observers (JM.S, L.R) for inter-observer variability analysis. To determine the intra-observer reproducibility, the same observer repeated measurements for the 10 randomly selected patients at least four weeks later. The coefficient of variation (CV), defined as the ratio of the standard deviation and the absolute mean and the intraclass

correlation coefficient (ICC) were estimated using Microsoft Excel Version 2016 (MS Excel 2016).

7.2.7 Statistical Analysis

Data from the study were analyzed using descriptive statistics. Quantitative results were expressed as mean and standard deviation, while qualitative or dichotomous variables were expressed as percentages. Chi-square test (χ^2) and Fisher's exact test were used, according to the size and characteristic of qualitative variables, to compare proportions and to study relationships between them. The comparison between two quantitative variables was made by the nonparametric Mann-Whitney U test. To estimate correlations between parameters, the Pearson and Spearman's Rho correlation coefficients were calculated as appropriate for the type of the data. A multiple linear regression was made to determine relationships and dependence between independent (clinical measures, laboratory and CMR parameters) and dependent (HFF and PFI) quantitative variables, which were related by previous steps. Data were analyzed using IBM SPSS Statistics for Windows, version 23.0 (IBM Corp., Armonk, N.Y.) and values of $p<0.05$ were considered significant.

7.3 Results

A total of 25 adolescents with obesity and 13 adolescents without obesity were included in our study. No subject was excluded, but HbA1c was not registered in seven subjects of the obese group and inflammatory parameters were not assessed in one

control subject and two obese subjects. No significant differences were found in demographic data and ethnicity (Table 1), except that non-obese subjects were slightly older, but every subject in both groups had Tanner stage 4-5. The main clinical and laboratory data are also expressed in Table 1. Both groups were well differentiated by obesity index and significant differences were found in BP, insulin resistance and dyslipidemia, while no adolescent was diagnosed with T2-DM. In the group of adolescents with obesity, the 60% were classified as systolic or diastolic high BP.

The data from the CMR evaluation are summarized in Table 2. Morbidly obese adolescents presented significant increases in the LV mass and volumes, however non-significant differences were observed in native T1 values (990.5 ms vs 1000.0 ms, p0.73). Additionally, significant increases were noted in the obese group in HFF (4.3% vs 10.8%, p0.03) and PFI (2.3 g/ht^3 vs 7.7 g/ht^3, $p<0.01$) (Figure 1).

Interestingly, significant gender-related differences were found in T1 and T2 mapping (Table 3), despite non-significant differences being observed between genders in demographic, clinical and laboratory data, except for SBP and hematocrit (Table 4). Females showed higher native T1 and T2 mean values than males, even when both genders were subclassified by obesity (Table 3), while non-significant differences were found in the remaining CMR parameters (Figure 2), with the exception of the significant increase in the males' LVMI. When obese and non-obese subjects were separately analysed by gender, significant differences were occasionally observed – especially in the PFI – and did not imply the T1 values (Table 5 and 6).

Subjects that met criteria for hypertension[16] showed significant differences in the LVMI and PFI, but not in the mapping parameters (Table 7).

On account of the differences observed between genders, the correlation analysis was performed with the whole sample and also independently by gender between the mapping values and the anthropometric, laboratory and CMR parameters (Table 8). In general, T1 and T2 mapping were inversely correlated with age, hematocrit and LVMI, highlighting the importance of these parameters in the acquisition and post-processing of T1 and T2 values, and positively correlated with PFI. In males, T1 values were correlated with the triponderal mass index (TMI) ($r = 0.51$, $p<0.05$), neutrophil levels ($r = 0.46$, $p<0.05$) and PFI ($r = 0.48$, $p<0.05$), while in females the native-T1s was correlated with HOMA-IR ($r = 0.49$, $p<0.05$).

The correlation analyses in HFF and PFI are shown in Table 9. HFF was well correlated in males with HOMA-IR ($r = 0.42$, p0.08) and inflammation cells and molecules (neutrophiles: $r = 0.58$, $p<0.05$) while non-significant correlation was found in females. PFI presented outstanding correlations with TMI ($r = 0.78$, $p<0.01$), BP ($r = 0.53$, $p<0.01$), HOMA-IR ($r = 0.56$, $p<0.01$) and hs-CRP ($r = 0.54$, $p<0.01$).

Considering the poor correlation results in mapping values in the whole cohort, multivariable regression models were considered only for HFF and PFI, without distinguishing between gender. In the unadjusted linear regression analysis to determine the best correlation for HFF, the final model ($R^2 = 0.33$ $p<0.0001$) showed HOMA-IR as the independent determinant (determinant coefficient: 1.58 [0.49-2.68], $p<0.01$), while for PFI, the final model ($R^2 = 0.76$ $p<0.0001$) resulted in TMI as the independent parameter (0.60 [0.43-0.77], $p<0.01$).

The intra-observer and inter-observer variability analysis for pericardial fat volume measurements had an acceptable reproducibility, with CV of 30% for both analyses and ICC of 0.95 and 0.90, respectively.

7.4 Discussion

The present study shows that morbidly obese adolescents present no differences in native T1 compared to non-obese adolescents, despite showing higher LV mass values. However, T1 and T2 mappings have notable gender-related differences, indicating structural or compositional myocardium peculiarities in females, with significantly higher values in both mapping measurements. In males, the native T1 values appear to be better correlated with obesity parameters, particularly with TMI and inflammatory cell levels. Similarly, the HFF and PFI are correlated with HOMA-IR, inflammatory parameters and TMI. These findings suggest the important role of inflammation and insulin resistance in the myocardial tissue modifications and the adipose tissue infiltration.

Obesity is a complex and multifactorial disease with multiple tissues affected as a consequence of metabolic pathway changes, adipose tissue infiltration and the endocrine and autocrine effect of pro-inflammatory molecules released by adipose tissue.[22] In the myocardium and blood vessels, obesity implies infiltration of adipocytes, macrophages and other white cells, resulting in angiogenesis, ECM remodeling, hypoxia and inflammation.[23] Macrophages play an important role in obesity-associated inflammation since they constitute the largest immune cell population in adipose tissue. Its switch from a M0-like to a M1-like phenotype triggers the release of

pro-inflammatory cytokines, such as tumor necrosis factor and interleukins 1 and 6, which exacerbate the immune system activation and induce insulin resistance.[17,22] Cardiac fibrosis and ECM remodeling are a consequence of the persistence of this inflammatory state.[24]

In obese subjects the value of native T1 time as indicator of myocardium ECM composition depends on the proportion and type of the cell infiltration in the myocardium. As a result of the cardiac steatosis, a decrease in native T1 value can be expected as occurs in the glycosphingolipid deposit of Fabry's disease.[25] Conversely, obesity also involves a low-grade inflammation state, fibrosis or reactive LV hypertrophy (LVH)[26] which might result in an increase of the native T1 time, as occurs in HCM, hypertension with LVH or myocarditis cases.[8,27,28] Lastly, dissimilar results have been shown in native T1 values of obese T2-DM patients.[11,29] Notably, most of the studies conducted in hypertension without LVH, diabetic or obese subjects have reported non-significant differences,[6] similar to our results.

Native T1 values in obese population have been only evaluated in two adult sample studies with dissimilar conclusions. Khan et al.[11] found non-significant differences in native T1 in obese diabetic adults compared to obese non-diabetic or healthy adults (944.0 vs 962.2 vs 985.5 ms), but showed a native T1 decrease in the obese diabetic and obese non-diabetic adults, which the authors attributed to myocardial steatosis. In contrast, Homsi et al.[12] also demonstrated non-significant differences in obese adults, which became a significant increase, attributed to myocardial fibrosis development, when only severely obese subjects were compared to non-obese controls (1010.5 vs 974.6 ms). The present study shows in obese

adolescents similar native T1 values to those reported in the latter obese adult study, and although statistical differences could not be demonstrated, the value noticed in the LV septum is in line with those observed in severely obese adults.

Most studies conducted in the pediatric population focused on children with HCM or myocarditis, and reported native T1 increases in HCM (1015-1020 ms)[27,30] and especially in myocarditis (1097 ms).[28] Control groups in these studies obtained native T1 times similar to our non-obese adolescents. Results indicate that native T1 is not useful to assess the degree of myocardial damage in obese adolescents. A possible explanation could be that native T1 is increased by the LV myocardium fibrosis or the ECM immune cell infiltration, but simultaneously attenuated by the adipose tissue myocardial infiltration, resulting in opposed values. Another explanation may relate to the robustness of the cell regeneration processes typical in early life, which would prevent fibrosis of the myocardium.[31] Nevertheless, we have found that native T1 times were correlated in males with neutrophil levels and TMI, an index especially useful in measuring cardiovascular risk in obese subjects,[32] while in females a correlation with insulin resistance could only be obtained in the LV septum study. Insulin and inflammation play an important role in obesity physiopathology,[10,33] however previous studies in obese subjects where mapping was tested focused on CMR parameters and BP, but lacked an evaluation of its relationships with inflammation and insulin resistance parameters.

Similarly, PFI was also found to be positively correlated with native T1 values. Pericardial adiposity is an indicator of adipose tissue expansion and has been demonstrated to be associated with metabolic and inflammatory markers, though less

than other measures of visceral adiposity including hepatic steatosis.[23,34] Our results showed that pericardial fat was strongly correlated with obesity indexes, such as BMI or TMI, and CV risk indicators as BP, HOMA-IR and hs-CRP. Similarly, hepatic steatosis was found to be positively correlated with insulin resistance and humoral and cellular inflammation, although the reported values of HFF in the obese group are placed in the liver steatosis grade I, according to the NASH-CRN scoring system.[35]

The gender-related significant differences in T1 and T2 mapping noticed in the present study (Table 3) is a cause for concern because it is unusual to differentiate between gender in mapping studies. Previous research conducted in adults found myocardial fibrosis to be more prevalent in females compared to males, related to the LV volume and mass decrease, although this was only demonstrated in the post-contrast T1 time and not in the native T1 time.[36] Additionally, other hypothesized explanations could be voluming blood pool when contouring the myocardium in thinner hearts and lower hematocrit values in women.[37-40] The correlation analysis in our study confirmed the importance of LVMI and hematocrit. Female hearts, significantly thinner than males, presented T1 and T2 values higher than male hearts, hence in our opinion both genders must be independently analyzed. Likewise, female adolescents between 12 and 18 year old present changes in their body composition, increasing their fat mass index by up to 10 points higher than male adolescents.[41] The increase observed in our study in HFF and PFI in non-obese females compared to males could be attributed to the difference in body composition.

This study has certain limitations. The cross-sectional design and small sample size limit the statistical strength of the conclusions. However, the two evaluated groups

were well differentiated and paired, and the techniques have been widely reproduced. Similarly, native T1 values in the control group are in the range reported in healthy children.[28,30] In addition, because no contrast agent was used, we were not able to evaluate the myocardial fibrosis impact and its relationship with native T1.

7.5 Conclusions

In summary, we have found native T1 is of limited use in differentiating obese adolescents at risk of myocardium ECM changes. Furthermore, we have shown a gender dimorphism in mapping values. Female adolescents possess particular characteristics such as thinner hearts and low hematocrit levels, which are associated with higher native T1 and T2 values. However in males, TMI is related to increased native T1 as well as pericardial fat, and may serve as a useful predictor. Therefore, a gender-individualized analysis must be implemented in future native T1 studies. Hepatic steatosis and pericardial fat are markers of adipose tissue infiltration closely related with high BP, insulin resistance and inflammation.

7.6 Tables and Figures

Table 1: Characteristic, clinical and laboratory data of study population: non-obese and obese adolescents.

Variable	Non-obese (N = 13)	Obese (N = 25)	P Value
Age (years)	15.6 ± 1.2	14.3 ± 1.4	**0.01**
Male	46%	52%	1
Ethnicity			0.39
Caucasian	92%	84%	
Latin American	0%	12%	
Asian	8%	4%	
BMI (kg/m^2)	20.2 ± 1.9	36.9 ± 5.9	**<0.01**
TMI (kg/m^3)	11.8 ± 1.1	22.3 ± 4.0	**<0.01**
SBP (mmHg)	110 ± 9	126 ± 10	**<0.01**
DBP (mmHg)	61 ± 5	72 ± 10	**<0.01**
Hypertension (≥90th percentile)	8%	60%	**<0.01**
Laboratory parameters			
Hematocrit (%)	41 ± 4	42 ± 2	0.56
Leucocyte (/µL)	6,884 ± 1,529	8,134 ± 1,727	**0.03**
Neutrophile (/µL)	3,736 ± 1,057	4,587 ± 1,220	**0.04**
Lymphocyte (/µL)	2,261 ± 659	2,587 ± 682	0.12
Platelet (/µL)	224,615 ± 54,234	281,541 ± 63,386	**<0.01**
Fasting glycemia (mg/dL)	72.3 ± 8.1	82.6 ± 7.6	**<0.01**
HbA1c (%) (N=31)	5.2 ± 0.1	5.3 ± 0.2	0.51
Insulin (µU/mL)	7.9 ± 4.3	29.0 ± 19.7	**<0.01**
HOMA-IR	1.4 ± 0.8	5.9 ± 4.1	**<0.01**
Lipid profile			
Total Cholesterol (mg/dL)	179 ± 22	170 ± 28	0.28
LDL-C (mg/dL)	106 ± 17	102 ± 21	0.41
HDL-C (mg/dL)	54 ± 7	43 ± 6	**<0.01**
Triglycerides (mg/dL)	73 ± 17	116 ± 62	**<0.01**
Inflammatory parameters (N = 36)			
hs-CRP (mg/dL)	0.05 ± 0.04	0.41 ± 0.55	**<0.01**
Interleukin 6 (pg/mL)	1.3 ± 1.3	3.5 ± 1.6	**<0.01**

Values expressed in mean and standard deviation; P value calculated by non-parametric Mann-Whitney U test; Dichotomous variables (Fisher's exact test); BMI, Body Mass Index; SD, Standard deviation; TMI, Triponderal Mass Index; SBP, Systolic blood pressure; DBP, Diastolic blood pressure; HbA1c, glycated hemoglobin; HOMA-IR, Homeostatic model assessment insulin resistance; LDL-C, cholesterol in low-density lipoprotein; HDL-C, cholesterol in high-density lipoprotein; hs-CRP, highly sensitive C-reactive protein.

Table 2: Cardiovascular magnetic resonance left ventricular measurements, mapping and cardiovascular magnetic resonance data of study population: non-obese and obese adolescents.

Variable	Non-obese (N = 13)	Obese (N = 25)	P Value
LVMI (g/ht^3)	22.9 ± 6.2	28.3 ± 4.7	**0.01**
LVEDVI (ml/m^2)	86.5 ± 15.6	71.9 ± 9.4	**<0.01**
LVESVI (ml/m^2)	35.0 ± 8.8	25.5 ± 6.0	**<0.01**
LVEF (%)	60.3 ± 4.1	63.6 ± 7.6	0.12
T1 mapping			
Native T1 (ms)	990.5 ± 31.2	1000.0 ± 28.5	0.73
Native-T1s (ms)	994.4 ± 37.0	1007.0 ± 31.1	0.28
Native-T1pw (ms)	986.6 ± 28.9	992.9 ± 39.2	0.92
T2 mapping (ms)	48.5 ± 2.9	46.8 ± 2.9	0.09
Pericardial Fat Index (g/ht^3)	2.3 ± 1.3	7.7 ± 2.3	**<0.01**
Hepatic Fat Fraction (%)	4.3 ± 3.5	10.8 ± 10.0	**0.03**

Values expressed in mean and standard deviation; P value calculated by non-parametric Mann-Whitney U test; Dichotomous variables (Fisher's exact test); LVMI, Left ventricular mass index; LVEDVI, Left ventricular end-diastolic volume index; LVESVI, Left ventricular end-systolic volume index; LVEF, Left ventricular ejection fraction; Native-T1s, Septal native T1; Native-T1pw, Posterior wall native T1.

Table 3: Cardiovascular magnetic resonance left ventricular measures, mapping and nuclear magnetic resonance data of study population classified by gender.

Variable	MALE			FEMALE			P VALUE Male vs Female		
	Non-obese (N = 6)	Obese (N = 13)	Total (N = 19)	Non-obese (N = 7)	Obese (N = 12)	Total (N = 19)	Non-obese	Obese	Total
LVMI (g/ht^3)	26.9 ± 4.0	29.4 ± 4.9	28.7 ± 4.6	19.4 ± 5.7	27.1 ± 4.4	24.3 ± 6.1	**0.03**	0.24	**0.03**
LVEDVI (ml/m^2)	97.6 ± 13.0	73.1 ± 11.1	80.9 ± 16.3	76.9 ± 10.9	70.6 ± 7.3	73.0 ± 9.1	**<0.01**	0.57	0.12
LVESVI (ml/m^2)	40.8 ± 9.3	25.1 ± 6.1	30.0 ± 10.2	29.9 ± 4.4	26.1 ± 6.1	27.5 ± 5.7	**0.01**	0.61	0.64
LVEF (%)	60.1 ± 4.6	65.1 ± 7.3	63.5 ± 6.8	60.5 ± 4.0	62.0 ± 7.8	61.4 ± 6.6	0.73	0.40	0.47
T1 mapping									
Native T1 (ms)	965.4 ± 22.8	987.8 ± 31.2	980.7 ± 30.1	1012.0 ± 18.8	1013.1 ± 18.8	1012.7 ± 18.3	**<0.01**	**0.02**	**<0.01**
Native-T1s (ms)	968.2 ± 23.2	989.1 ± 26.2	982.5 ± 26.6	1016.9 ± 31.9	1026.5 ± 24.0	1022.9 ± 26.7	**<0.01**	**<0.01**	**<0.01**
Native-T1pw (ms)	962.6 ± 24.3	986.6 ± 42.3	979.0 ± 38.5	1007.1 ± 10.7	999.8 ± 36.2	1002.5 ± 29.2	**<0.01**	0.32	**0.02**
T2 mapping (ms)	45.8 ± 1.5	45.6 ± 3.0	45.7 ± 2.6	50.8 ± 1.5	48.2 ± 2.2	49.1 ± 2.3	**<0.01**	**0.02**	**<0.01**
Pericardial Fat Index (g/ht^3)	1.6 ± 1.0	7.5 ± 2.4	5.6 ± 3.4	2.8 ± 1.3	7.9 ± 2.4	6.0 ± 3.2	0.13	0.47	0.70
Hepatic Fat Fraction (%)	2.3 ± 1.6	9.3 ± 8.5	7.0 ± 7.7	6.0 ± 3.9	12.3 ± 11.5	10.0 ± 9.7	**0.01**	0.37	0.07

Values expressed in mean and standard deviation; P value calculated by non-parametric Mann-Whitney U test; Dichotomous variables (Fisher's exact test); LVMI, Left ventricular mass index; LVEDVI, Left ventricular end-diastolic volume index; LVESVI, Left ventricular end-systolic volume index; LVEF, Left ventricular ejection fraction; Native-T1s, Septal native T1; Native-T1pw, Posterior wall native T1.

Table 4: Characteristic, clinical and laboratory data of study population classified by gender.

Variable	Male (N = 19)	Female (N = 19)	P Value
Age (years)	15.0 ± 1.4	14.5 ± 1.5	0.50
BMI (kg/m^2)	31.0 ± 8.0	31.3 ± 10.9	0.97
TMI (kg/m^3)	17.9 ± 5.0	19.5 ± 6.9	0.40
SBP (mmHg)	126 ± 12	116 ± 11	**0.02**
DBP (mmHg)	68 ± 9	68 ± 11	0.95
Hypertension (≥90th percentile)	47%	37%	0.74
Laboratory parameters			
Hematocrit (%)	43 ± 2	40 ± 3	**0.02**
Leucocyte (/µL)	7,878 ± 1,827	7,534 ± 1,696	0.48
Neutrophile (/µL)	4,353 ± 1,229	4,238 ± 1,247	0.64
Lymphocyte (/µL)	2,523 ± 698	2,428 ± 685	0.75
Platelet (/µL)	257,684 ± 62,496	265,611 ± 70,355	1
Fasting glycemia (mg/dL)	81.6 ± 8.6	76.6 ± 9.1	0.09
HbA1c (%) (N = 31)	5.3 ± 0.2	5.2 ± 0.1	0.23
Insulin (µU/mL)	21.2 ± 14.7	22.4 ± 22.8	0.77
HOMA-IR	4.4 ± 3.2	4.4 ± 4.8	0.77
Lipid profile			
Total Cholesterol (mg/dL)	174 ± 30	172 ± 21	0.97
LDL-C (mg/dL)	106 ± 23	101 ± 16	0.70
HDL-C (mg/dL)	45 ± 7	49 ± 9	0.29
Triglycerides (mg/dL)	115 ± 73	88 ± 24	0.52
Inflammatory parameters (N = 36)			
hs-CRP (mg/dL)	0.22 ± 0.24	0.34 ± 0.61	0.85
Interleukin 6 (pg/mL)	2.6 ± 1.9	2.8 ± 1.8	0.66

Values expressed in mean and standard deviation; P value calculated by non-parametric Mann-Whitney U test; Dichotomous variables (Fisher's exact test); BMI, Body Mass Index; TMI, Triponderal Mass Index; SBP, Systolic blood pressure; DBP, Diastolic blood pressure; HbA1c, glycated hemoglobin; HOMA-IR, Homeostatic model assessment insulin resistance; LDL-C, cholesterol in low-density lipoprotein; HDL-C, cholesterol in high-density lipoprotein; hs-CRP, highly sensitive C-reactive protein.

Table 5: Specific data in males. Cardiovascular magnetic resonance, mapping, pericardial fat and hepatic fat data.

Variable	Male Non-obese (N = 6)	Male Obese (N = 13)	P Value
LVMI (g/ht^3)	26.9 ± 4.0	29.4 ± 4.9	0.46
LVEDVI (ml/m^2)	97.6 ± 13.0	73.1 ± 11.1	**<0.01**
LVESVI (ml/m^2)	40.8 ± 9.3	25.1 ± 6.1	**<0.01**
LVEF (%)	60.1 ± 4.6	65.1 ± 7.3	0.15
T1 mapping			
Native T1 (ms)	965.4 ± 22.8	987.8 ± 31.2	0.32
Native-T1s (ms)	968.2 ± 23.2	989.1 ± 26.2	0.17
Native-T1pw (ms)	962.6 ± 24.3	986.6 ± 42.3	0.28
T2 mapping (ms)	45.8 ± 1.5	45.6 ± 3.0	0.52
Hepatic Fat Fraction (%)	2.3 ± 1.6	9.3 ± 8.5	0.06
Pericardial Fat Index (g/ht^3)	1.6 ± 1.0	7.5 ± 2.4	**<0.01**

LVMI, Left ventricular mass index; LVEDVI, Left ventricular end-diastolic volume index; LVESVI, Left ventricular end-systolic volume index; LVEF, Left ventricular ejection fraction; Native-T1s, Septal native T1; Native-T1pw, Posterior wall native T1.

Table 6: Specific data in females. Cardiovascular magnetic resonance, mapping, pericardial fat and hepatic fat data.

Variable	Female Non-obese (N = 7)	Female Obese (N = 12)	P Value
LVMI (g/ht^3)	19.4 ± 5.7	27.1 ± 4.4	**0.01**
LVEDVI (ml/m^2)	76.9 ± 10.9	70.6 ± 7.3	0.16
LVESVI (ml/m^2)	29.9 ± 4.4	26.1 ± 6.1	0.10
LVEF (%)	60.5 ± 4.0	62.0 ± 7.8	0.59
T1 mapping			
Native T1 (ms)	1012.0 ± 18.8	1013.1 ± 18.8	0.38
Native-T1s (ms)	1016.9 ± 31.9	1026.5 ± 24.0	0.43
Native-T1pw (ms)	1007.1 ± 10.7	999.8 ± 36.2	0.22
T2 mapping (ms)	50.8 ± 1.5	48.2 ± 2.2	**<0.01**
Hepatic Fat Fraction (%)	6.0 ± 3.9	12.3 ± 11.5	0.22
Pericardial Fat Index (g/ht^3)	2.8 ± 1.3	7.9 ± 2.4	**<0.01**

LVMI, Left ventricular mass index; LVEDVI, Left ventricular end-diastolic volume index; LVESVI, Left ventricular end-systolic volume index; LVEF, Left ventricular ejection fraction; Native-T1s, Septal native T1; Native-T1pw, Posterior wall native T1.

Table 7: Characteristic, mapping and cardiovascular magnetic resonance (CMR) parameters of study population classified by criteria of hypertension (blood pressure ≥90th percentile).

Variable	No Hypertension (N = 22)	Hypertension (N = 16)	P Value
Age (years)	15.1 ± 1.5	14.2 ± 1.2	**0.03**
BMI (kg/m^2)	27.3 ± 8.3	36.5 ± 8.3	**<0.01**
TMI (kg/m^3)	16.3 ± 5.5	22.0 ± 5.2	**<0.01**
CMR parameters			
LVMI (gr/ht^3)	24.5 ± 5.7	29.2 ± 4.8	**0.02**
LVEDVI (ml/m^2)	80.8 ± 15.8	71.6 ± 7.4	0.06
LVESVI (ml/m^2)	31.3 ± 9.0	25.3 ± 5.8	**0.02**
LVEF (%)	61.8 ± 5.5	63.5 ± 8.2	0.29
Native T1 (ms)	994.2 ± 32.4	1000.2 ± 25.3	0.73
Native-T1s (ms)	999.3 ± 37.2	1007.4 ± 27.6	0.47
Native-T1pw (ms)	989.1 ± 35.0	993.0 ± 37.8	0.69
T2 mapping (ms)	47.6 ± 3.1	47.2 ± 2.9	0.60
Pericardial Fat Index (g/ht^3)	4.4 ± 3.0	7.7 ± 2.7	**<0.01**
Hepatic Fat Fraction (%)	6.8 ± 7.9	11.0 ± 9.8	0.12

Values expressed in mean and standard deviation; P value calculated by non-parametric Mann-Whitney U test; BMI, Body Mass Index; TMI, Triponderal Mass Index; LVMI, Left ventricular mass index; LVEDVI, Left ventricular end-diastolic volume index; LVESVI, Left ventricular end-systolic volume index; LVEF, Left ventricular ejection fraction; Native-T1s, Septal native T1; Native-T1pw, Posterior wall native T1.

Table 8: Bivariate correlations of mapping values with clinical, laboratory and cardiovascular magnetic resonance (CMR) parameters. Analysis performed in the total cohort, as well as independently in males (M) and females (F).

Variable	Native T1			Native-T1s			Native-T1pw			T2 mapping		
	Total	**M**	**F**	**Total**	**M**	**F**	**Total**	**M**	**F**	**Total**	**M**	**F**
Age	-0.34†	-0.57†	0.03	-0.38†	-0.56†	-0.19	-0.22	-0.49†	0.28	-0.09	-0.26	0.15
BMI	0.09	0.43	-0.34	0.17	0.44†	-0.06	0.05	0.40	-0.36	-0.12	0.00	-0.52†
TMI	0.20	0.51†	-0.35	0.32	0.59*	-0.05	0.12	0.44	-0.39	-0.01	0.02	-0.47†
SBP	-0.12	0.24	-0.19	-0.09	0.43	-0.13	-0.07	0.16	-0.10	-0.22	0.41	-0.50†
DBP	0.13	0.17	0.03	0.22	0.31	-0.07	0.06	0.21	0.02	0.09	0.28	-0.17
Laboratory												
HOMA-IR	0.19	0.26	0.07	0.28	0.27	0.49†	0.09	0.18	-0.15	-0.19	-0.06	-0.48†
Hematocrit	-0.46*	-0.36	-0.29	-0.35†	-0.32	0.15	-0.40†	-0.34	-0.34	-0.51*	-0.45†	-0.36
Leukocytes	0.02	0.29	0.04	0.04	0.16	0.29	0.00	0.31	-0.23	-0.30	-0.40	-0.07
Neutrophile	0.18	0.46†	0.16	0.14	0.30	0.23	0.19	0.52†	-0.06	-0.06	-0.14	0.10
Lymphocyte	0.02	0.32	-0.16	0.11	0.26	0.37	-0.10	0.22	-0.42	-0.31	-0.28	-0.44
hs-CRP	0.05	-0.00	-0.23	0.11	0.03	0.07	0.01	0.03	-0.25	-0.10	-0.02	-0.48†
Interleukin 6	0.22	0.28	-0.04	0.27	0.29	0.10	0.18	0.31	0.01	0.02	0.05	-0.26
CMR												
LVMI	-0.33†	-0.19	-0.19	-0.24	0.04	-0.12	-0.30	-0.26	-0.25	-0.50*	-0.26	-0.58*
LVEF	0.05	0.14	0.08	0.08	0.18	0.14	0.04	0.15	-0.10	-0.03	0.10	-0.03
PFI	0.23	0.48†	-0.32	0.36†	0.52†	0.14	0.17	0.50†	-0.43	-0.15	0.12	-0.67*
HFF	0.24	0.35	-0.18	0.28	0.11	0.28	0.14	0.34	-0.39	0.08	0.00	-0.22

Spearman coefficients. Values expressed in r. *p<0.01. †p<0.05. M, Male; F, Female; Native T1, global native T1 value in short-axis; Native-T1s, native T1 value in LV septum; Native-T1pw, native T1 value in LV posterior wall; BMI, Body Mass Index; TMI, Triponderal Mass Index; SBP, Systolic Blood Pressure; DBP, Diastolic Blood Pressure; HOMA-IR, Homeostatic model assessment insulin resistance; hs-CRP, highly sensitive C-reactive protein; CMR, cardiovascular magnetic resonance; LVMI, Left ventricular mass index; LVEF, Left ventricular ejection fraction; HFF, Hepatic Fat Fraction; PFI, Pericardial fat index.

Table 9: Bivariate correlations of hepatic fat fraction and pericardial fat index with clinical, laboratory and cardiovascular magnetic resonance (CMR) parameters. Analysis performed in the total cohort, as well as independently in males (M) and females (F).

Variable	Hepatic Fat Fraction			Pericardial Fat Index		
	Total	**M**	**F**	**Total**	**M**	**F**
Age	-0.27	-0.21	-0.32	-0.59*	-0.71*	-0.40
BMI	0.29	0.43	0.14	0.79*	0.75*	0.76*
TMI	0.29	0.32	0.12	0.78*	0.77*	0.75*
SBP	0.05	0.16	0.17	0.53*	0.68*	0.52†
DBP	0.05	0.01	0.11	0.47*	0.55†	0.20
Laboratory						
HOMA-IR	0.33†	0.42	0.27	0.56*	0.55†	0.54†
Hematocrit	-0.01	-0.17	0.27	-0.02	-0.16	0.16
Leukocytes	0.24	0.52†	0.08	0.20	0.08	0.10
Neutrophile	0.30	0.58†	0.10	0.22	0.36	-0.07
Lymphocyte	0.12	0.26	0.01	0.23	0.00	0.43
hs-CRP	0.48*	0.49†	0.43	0.54*	0.54†	0.51†
Interleukin 6	0.28	0.45	0.04	0.52*	0.61*	0.28
CMR						
LVMI	-0.09	-0.44	0.34	0.36†	0.03	0.72*
LVEF	-0.09	-0.22	0.23	0.24	0.51†	0.00
PFI	0.25	0.23	0.19	1	1	1
HFF	1	1	1	0.25	0.23	0.19

Spearman coefficients. Values expressed in r. *p<0.01. †p<0.05. M, Male; F, Female; BMI, Body Mass Index; TMI, Triponderal Mass Index; SBP, Systolic Blood Pressure; DBP, Diastolic Blood Pressure; HOMA-IR, Homeostatic model assessment insulin resistance; hs-CRP, highly sensitive C-reactive protein; CMR, cardiovascular magnetic resonance; LVMI, Left ventricular mass index; LVEF, Left ventricular ejection fraction. HFF, Hepatic Fat Fraction; PFI, Pericardial fat index.

Figure 1: Box-and-whisker plots (median and 25-75th percentile) of mapping values and tissue fat determinations by study groups.

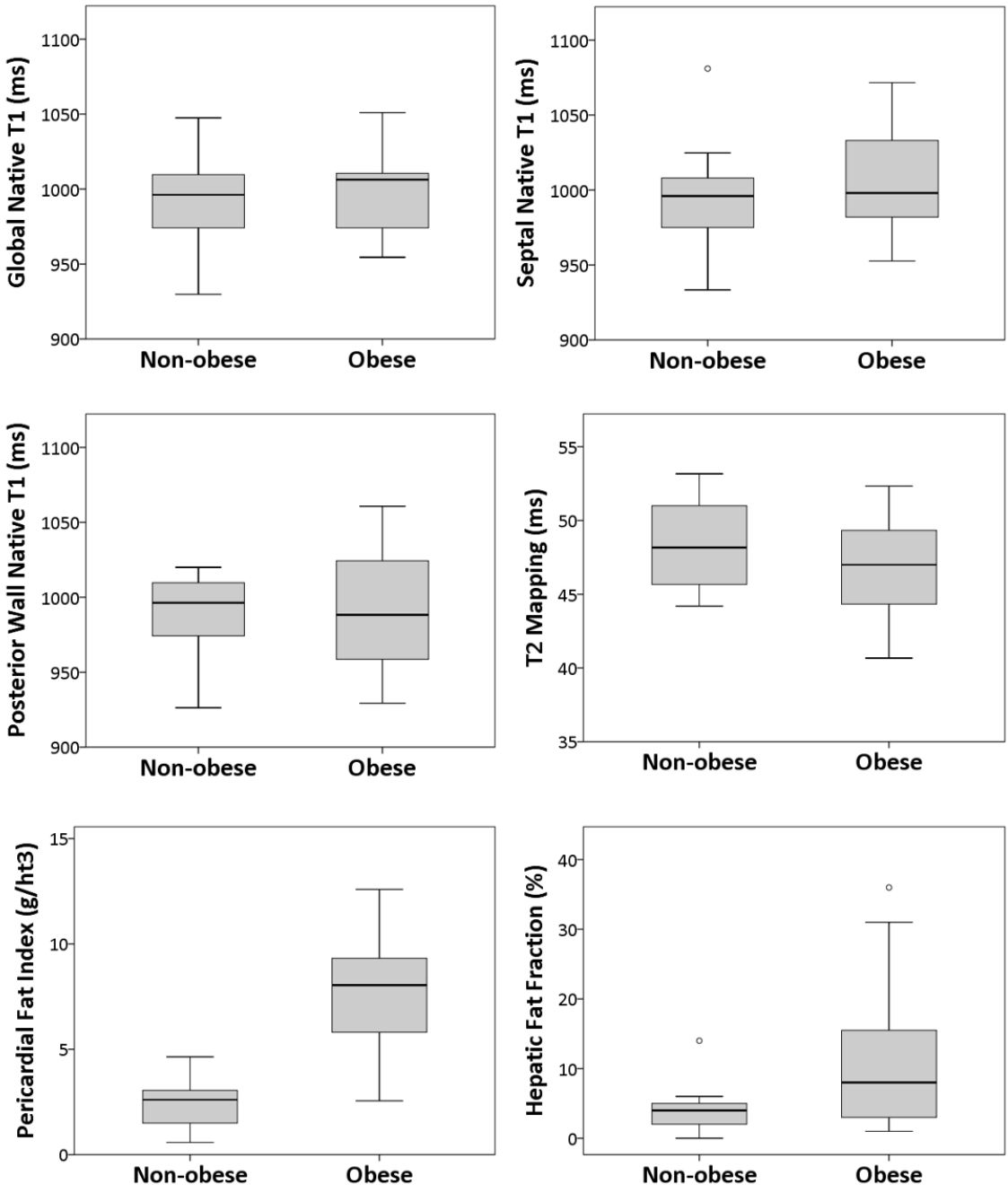

Figure 2: Box-and-whisker plots (median and 25-75th percentile) of mapping values and tissue fat determinations by study groups and gender: male (striped) and female (solid).

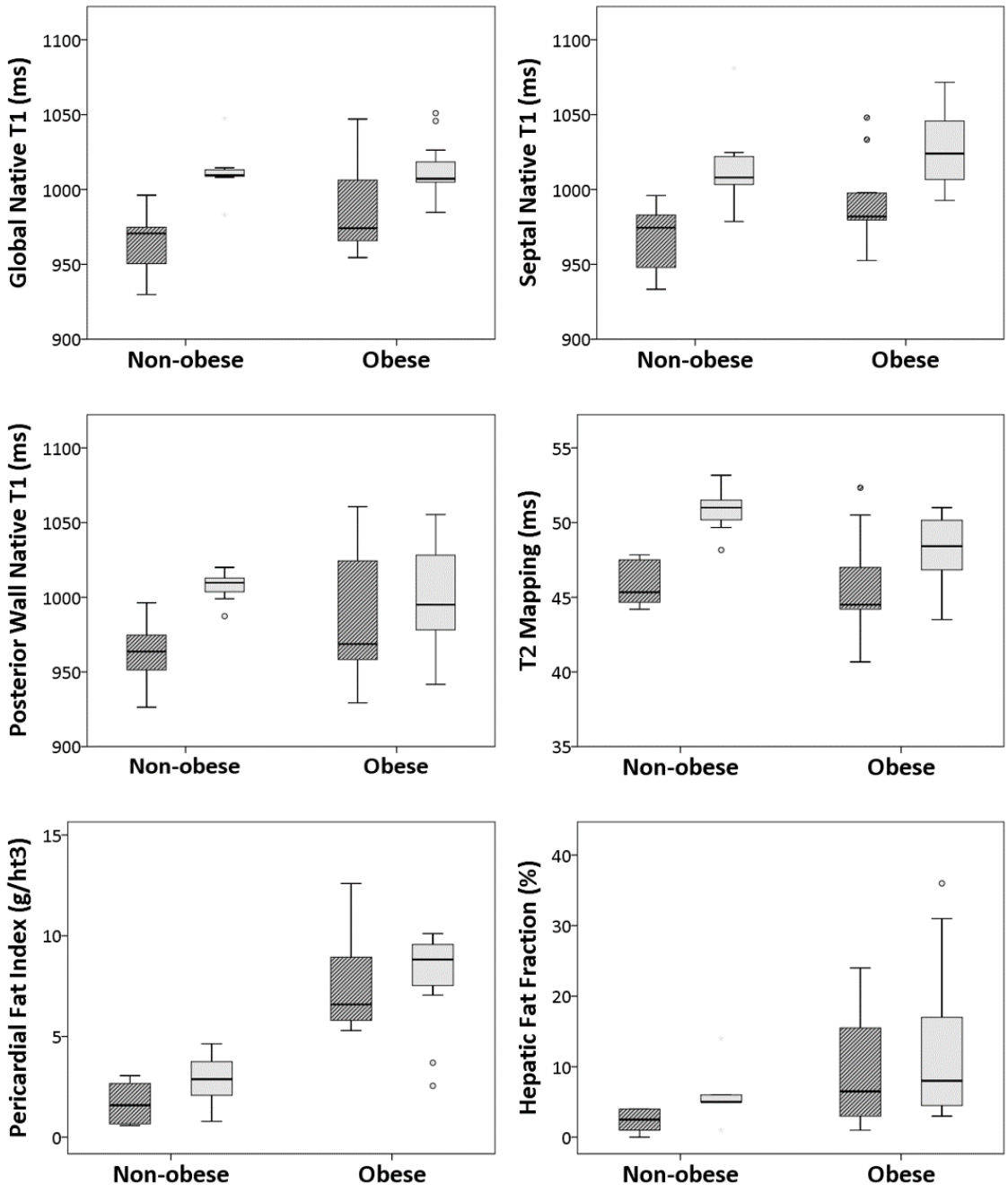

8. CONCLUSIONS

Each of the next specific conclusions refers to the specific aims on the “Hypothesis and Aims” section and on the same order:

1. Morbidly obese adolescents have an abnormal left ventricular geometry and systolic and diastolic LV dysfunctions, only detected by strain techniques, even when primary comorbidities, such as diabetes mellitus, have not yet been diagnosed.
2. Those obese adolescents labeled as metabolically healthy, despite exhibiting better BMI, blood pressure, insulin resistance and lipid profile, present the same pathological left ventricular changes than those metabolically unhealthy.
3. Morbidly obese adolescents present an atherosclerotic lipoprotein particle profile despite showing no pathological concentrations in the conventional lipid profile. The advanced lipoprotein test and the glycoprotein A inflammatory marker appear to provide more reliable indicators of cardiac change severity in obese adolescents than traditional CV risk factors such as BMI, blood pressure and insulin resistance.
4. Morbidly obese adolescents present native T1 values similar to non-obese adolescents, therefore native T1 appears to be of limited use in measuring the

risk of myocardium ECM changes in obesity. However, a gender dimorphism in mapping values has been noticed. Female adolescents possess particular characteristics such as thinner hearts and low hematocrit levels, which are associated with higher native T1 and T2 values, whereas in males, TMI is related to increased native T1 as well as pericardial fat, and may serve as a useful predictor. Therefore, a gender-individualized analysis must be implemented in future native T1 studies.

5. Hepatic steatosis and pericardial fat are markers of adipose tissue infiltration closely related with high BP, insulin resistance and inflammation.

Overall, this project has shown that morbidly obese adolescents prematurely present left ventricular hypertrophy and dysfunction, which are primarily tested using advanced echocardiographic techniques. However, contrary to our hypothesis, these changes do not coincide with quantifiable modifications in the myocardial extracellular matrix, which is possibly explained because of the simultaneous myocardium fibrosis and adipose tissue infiltration effects. In my experience, these patients are rarely evaluated by cardiologists or, when this does happen, only the left ventricular mass index is considered. However, these studies show that myocardial adaptive changes frequently affect myocardial structure as well as function and are independent of the diagnosis of comorbidities, so omitting cardiac evaluation for any adolescent with morbid obesity misses the opportunity to identify early cardiac damage.

Interestingly, the relationship found between the degree of cardiac involvement and a characteristic inflammatory and atherosclerotic lipoprotein particle profile opens

the possibility of using these novel markers as differentiating factors for predicting cardiac damage in these patients.

9. REFERENCES

9.1 Introduction and Methodology

1. World Health Organization. Obesity and overweight. https://www.who.int/mediacentre/factsheets/fs311/en/ (2016)
2. Blüher M. Metabolically Healthy Obesity. Endocr Rev. 2020;41(3):405-420.
3. Garrido-Miguel M, Cavero-Redondo I, Álvarez-Bueno C et al. Prevalence and Trends of Overweight and Obesity in European Children From 1999 to 2016: A Systematic Review and Meta-analysis. JAMA Pediatr. 2019;173(10):e192430.
4. Eckel N, Li Y, Kuxhaus O, Stefan N, Hu FB, Schulze MB. Transition from metabolic healthy to unhealthy phenotypes and association with cardiovascular disease risk across BMI categories in 90 257 women (the Nurses' Health Study): 30 year follow-up from a prospective cohort study. Lancet Diabetes Endocrinol. 2018;6(9):714–724.
5. Lavie CJ, Laddu D, Arena R, Ortega FB, Alpert MA, Kushner RF. Healthy weight and obesity prevention: JACC health promotion series. J Am Coll Cardiol. 2018;72(13):1506–1531.
6. van Vliet-Ostaptchouk JV, Nuotio ML, Slagter SN, et al. The prevalence of metabolic syndrome and metabolically healthy obesity in Europe: a collaborative analysis of

ten large cohort studies. BMC Endocr Disord. 2014;14:9.

7. Damanhoury S, Newton AS, Rashid M, Hartling L, Byrne JLS, Ball GDC. Defining metabolically healthy obesity in children: a scoping review. Obes Rev. 2018;19(11):1476-1491.
8. Yeste D, Clemente M, Campos A et al. Diagnostic accuracy of the tri-ponderal mass index in identifying the unhealthy metabolic obese phenotype in obese patients. An Pediatr (Barc). 2020;S1695-4033(20)30149-1.
9. Stefan N, Häring HU, Hu FB, Schulze MB. Metabolically healthy obesity: epidemiology, mechanisms, and clinical implications. Lancet Diabetes Endocrinol. 2013;1(2):152-62.
10. Corica D, Oreto L, Pepe G et al. Precocious Preclinical Cardiovascular Sonographic Markers in Metabolically Healthy and Unhealthy Childhood Obesity. Front Endocrinol (Lausanne). 2020;11:56.
11. World Health Organization. (2020). Global health estimates. http://www.who.int/healthinfo/global_health_estimates/en/ [Accessed December 15, 2021].
12. Borén J, Chapman MJ, Krauss RM et al. Low-density lipoproteins cause atherosclerotic cardiovascular disease: pathophysiological, genetic, and therapeutic insights: a consensus statement from the European Atherosclerosis Society Consensus Panel. Eur Heart J (2020) 41(24):2313-2330
13. Emerging Risk Factors Collaboration, Di Angelantonio E, Sarwar N, Perry P et al. Major lipids, apolipoproteins, and risk of vascular disease. JAMA (2009) 302:1993-2000

14. Varbo A, Benn M, Smith GD, Timpson NJ, Tybjaerg-Hansen A, Nordestgaard BG. Remnant cholesterol, low-density lipoprotein cholesterol, and blood pressure as mediators from obesity to ischemic heart disease. Circ Res (2015) 116:665-73
15. Varbo A, Freiberg JJ, Nordestgaard BG. Remnant Cholesterol and Myocardial Infarction in Normal Weight, Overweight, and Obese Individuals from the Copenhagen General Population Study. Clin Chem (2018) 64(1):219-230
16. Cromwell WC, Otvos JD, Keyes MJ et al. LDL Particle Number and Risk of Future Cardiovascular Disease in the Framingham Offspring Study - Implications for LDL Management. J Clin Lipidol (2007) 1:583-92
17. Davidson MH, Ballantyne CM, Jacobson TA et al. Clinical utility of inflammatory markers and advanced lipoprotein testing: advice from an expert panel of lipid specialists. J Clin Lipidol (2011) 5(5):338-67
18. Girona J, Amigó N, Ibarretxe D et al. HDL Triglycerides: A New Marker of Metabolic and Cardiovascular Risk. Int J Mol Sci (2019) 20(13):3151.
19. Fernández-Cidón B, Candás-Estébanez B, Gil-Serret M et al. Physicochemical properties of lipoproteins assessed by nuclear magnetic resonance as a predictor of premature cardiovascular disease. PRESARV-SEA study. J Clin Med (2021) 10(7):1379.
20. Pichler G, Amigo N, Tellez-Plaza M et al. LDL particle size and composition and incident cardiovascular disease in a South-European population: The Hortega-Liposcale Follow-up Study. Int J Cardiol (2018) 264:172-178.
21. Mora S, Buring JE, Ridker PM. Discordance of low-density lipoprotein (LDL) cholesterol with alternative LDL-related measures and future coronary events. Circulation (2014) 129(5):553-61.

22. Tehrani DM, Zhao Y, Blaha MJ et al. Discordance of Low-Density Lipoprotein and High-Density Lipoprotein Cholesterol Particle Versus Cholesterol Concentration for the Prediction of Cardiovascular Disease in Patients With Metabolic Syndrome and Diabetes Mellitus (from the Multi-Ethnic Study of Atherosclerosis [MESA]). Am J Cardiol (2016) 117(12):1921-7.
23. Urbina EM, McCoy CE, Gao Z et al. Lipoprotein particle number and size predict vascular structure and function better than traditional lipids in adolescents and young adults. J Clin Lipidol (2017) 11(4):1023-1031.
24. Mackey RH, McTigue KM, Chang YF et al. Lipoprotein particles and size, total and high molecular weight adiponectin, and leptin in relation to incident coronary heart disease among severely obese postmenopausal women: The Women's Health Initiative Observational Study. BBA Clin (2015) 3:243-250.
25. Mora S, Caulfield MP, Wohlgemuth J et al. Atherogenic Lipoprotein Subfractions Determined by Ion Mobility and First Cardiovascular Events After Random Allocation to High-Intensity Statin or Placebo: The Justification for the Use of Statins in Prevention: An Intervention Trial Evaluating Rosuvastatin (JUPITER) Trial. Circulation (2015) 132(23):2220-9.
26. Eckel N, Meidtner K, Kalle-Uhlmann T, Stefan N, Schulze MB. Metabolically healthy obesity and cardiovascular events: a systematic review and metanalysis. Eur J Prev Cardiol. 2016;23(9):956–966.
27. Norris AL, Steinberger J, Steffen LM, Metzig AM, Schwarzenberg SJ, Kelly AS. Circulating oxidized LDL and inflammation in extreme pediatric obesity. Obesity (Silver Spring). 2011;19(7):1415-9.
28. Krumholz HM, Larson M, Levy D. Prognosis of left ventricular geometric patterns in

the Framingham Heart Study. J Am Coll Cardiol. 1995;25(4):879-84.

29. Di Bonito P, Moio N, Sibilio G et al. Cardiometabolic phenotype in children with obesity. J Pediatr. 2014;165(6):1184-9.
30. Singh GK, Cupps B, Pasque M, Woodard PK, Holland MR, Ludomirsky A. Accuracy and reproducibility of strain by speckle tracking in pediatric subjects with normal heart and single ventricular physiology: a two-dimensional speckle-tracking echocardiography and magnetic resonance imaging correlative study. J Am Soc Echocardiogr. 2010;23(11):1143-52.
31. Patel MD, Myers C, Negishi K, Singh GK, Anwar S. Two-Dimensional Strain is more Precise than Conventional Measures of Left Ventricular Systolic Function in Pediatric Patients. Pediatr Cardiol. 2020;41(1):186-193.
32. Norris AL, Steinberger J, Steffen LM, Metzig AM, Schwarzenberg SJ, Kelly AS. Circulating oxidized LDL and inflammation in extreme pediatric obesity. Obesity (Silver Spring). 2011;19(7):1415-9.
33. Weiss R, Dziura J, Burgert TS et al. Obesity and the metabolic syndrome in children and adolescents. N Engl J Med. 2004;350(23):2362-74.
34. Ogorodnikova AD, Kim M, McGinn AP, Muntner P, Khan U, Wildman RP. Incident cardiovascular disease events in metabolically benign obese individuals. Obesity. 2012;20:651–9.
35. Maron BJ, Towbin JA, Thiene G et al. Contemporary definitions and classification of the cardiomyopathies: an American Heart Association Scientific Statement from the Council on Clinical Cardiology, Heart Failure and Transplantation Committee; Quality of Care and Outcomes Research and Functional Genomics and Translational Biology Interdisciplinary Working Groups; and Council on

Epidemiology and Prevention. Circulation. 2006;113(14):1807-16.

36. Weber KT, Jalil JE, Janicki JS, Pick R. Myocardial collagen remodeling in pressure overload hypertrophy. A case for interstitial heart disease. Am J Hypertens. 1989;2(12 Pt 1):931-40.
37. Taylor AJ, Salerno M, Dharmakumar R, Jerosch-Herold M. T1 Mapping: Basic Techniques and Clinical Applications. JACC Cardiovasc Imaging. 2016;9(1):67-81.
38. Jellis CL, Kwon DH. Myocardial T1 mapping: modalities and clinical applications. Cardiovasc Diagn Ther. 2014;4(2):126–137
39. Aherne E, Chow K, Carr J. Cardiac T1 mapping: Techniques and applications. J Magn Reson Imaging. 2020;51(5):1336-1356.
40. van den Boomen M, Slart RHJA, Hulleman EV et al. Native T1 reference values for nonischemic cardiomyopathies and populations with increased cardiovascular risk: A systematic review and meta-analysis. J Magn Reson Imaging. 2018;47(4):891-912.
41. Puntmann VO, Carr-White G, Jabbour A et al; International T1 Multicentre CMR Outcome Study. T1-Mapping and Outcome in Nonischemic Cardiomyopathy: All-Cause Mortality and Heart Failure. JACC Cardiovasc Imaging. 2016;9(1):40-50.
42. Rodrigues JC, Amadu AM, Ghosh Dastidar A et al. ECG strain pattern in hypertension is associated with myocardial cellular expansion and diffuse interstitial fibrosis: a multi-parametric cardiac magnetic resonance study. Eur Heart J Cardiovasc Imaging. 2017;18(4):441-450.
43. Germain P, El Ghannudi S, Jeung MY et al. Native T1 mapping of the heart - a pictorial review. Clin Med Insights Cardiol. 2014;8(Suppl 4):1-11.
44. Hotamisligil GS. Inflammation, metaflammation and immunometabolic disorders.

Nature. 2017 Feb 8;542(7640):177-185.

45. Khan JN, Wilmot EG, Leggate M et al. Subclinical diastolic dysfunction in young adults with Type 2 diabetes mellitus: a multiparametric contrast-enhanced cardiovascular magnetic resonance pilot study assessing potential mechanisms. Eur Heart J Cardiovasc Imaging. 2014;15(11):1263-9.
46. Homsi R, Yuecel S, Schlesinger-Irsch U et al. Epicardial fat, left ventricular strain, and T1-relaxation times in obese individuals with a normal ejection fraction. Acta Radiol. 2019;60(10):1251-1257.
47. Toemen L, Santos S, Roest AAW et al. Pericardial adipose tissue, cardiac structures, and cardiovascular risk factors in school-age children. Eur Heart J Cardiovasc Imaging. 2021;22(3):307-313.
48. Carrascosa A, Yeste D, Moreno-Galdo A, Gussinye M, Ferrandez A, Clemente M, Fernandez-Cancio M. Body mass index and tri-ponderal mass index of 1,453 healthy non-obese, non-undernourished millennial children. The Barcelona longitudinal growth study. An Pediatr (Bar) 2018;89:137–143.
49. Prakken NH, Velthuis BK, Teske AJ, Mosterd A, Mali WP, Cramer MJ. Cardiac MRI reference values for athletes and nonathletes corrected for body surface area, training hours/week and sex. Eur J Cardiovasc Prev Rehabil 2010;17:198–203.

9.2 Lipoprotein Particle Profile and Cardiac Involvement Study

1. Borén J, Chapman MJ, Krauss RM et al. Low-density lipoproteins cause atherosclerotic cardiovascular disease: pathophysiological, genetic, and therapeutic insights: a consensus statement from the European Atherosclerosis Society Consensus Panel. Eur Heart J (2020) 41(24):2313-2330
2. Emerging Risk Factors Collaboration, Di Angelantonio E, Sarwar N, Perry P et al. Major lipids, apolipoproteins, and risk of vascular disease. JAMA (2009) 302:1993-2000
3. Varbo A, Benn M, Smith GD, Timpson NJ, Tybjaerg-Hansen A, Nordestgaard BG. Remnant cholesterol, low-density lipoprotein cholesterol, and blood pressure as mediators from obesity to ischemic heart disease. Circ Res (2015) 116:665-73
4. Varbo A, Freiberg JJ, Nordestgaard BG. Remnant Cholesterol and Myocardial Infarction in Normal Weight, Overweight, and Obese Individuals from the Copenhagen General Population Study. Clin Chem (2018) 64(1):219-230
5. Cromwell WC, Otvos JD, Keyes MJ et al. LDL Particle Number and Risk of Future Cardiovascular Disease in the Framingham Offspring Study - Implications for LDL Management. J Clin Lipidol (2007) 1:583-92
6. Davidson MH, Ballantyne CM, Jacobson TA et al. Clinical utility of inflammatory markers and advanced lipoprotein testing: advice from an expert panel of lipid specialists. J Clin Lipidol (2011) 5(5):338-67
7. Girona J, Amigó N, Ibarretxe D et al. HDL Triglycerides: A New Marker of Metabolic and Cardiovascular Risk. Int J Mol Sci (2019) 20(13):3151.

8. Fernández-Cidón B, Candás-Estébanez B, Gil-Serret M et al. Physicochemical properties of lipoproteins assessed by nuclear magnetic resonance as a predictor of premature cardiovascular disease. PRESARV-SEA study. J Clin Med (2021) 10(7):1379.
9. Pichler G, Amigo N, Tellez-Plaza M et al. LDL particle size and composition and incident cardiovascular disease in a South-European population: The Hortega-Liposcale Follow-up Study. Int J Cardiol (2018) 264:172-178.
10. Mora S, Buring JE, Ridker PM. Discordance of low-density lipoprotein (LDL) cholesterol with alternative LDL-related measures and future coronary events. Circulation (2014) 129(5):553-61.
11. Tehrani DM, Zhao Y, Blaha MJ et al. Discordance of Low-Density Lipoprotein and High-Density Lipoprotein Cholesterol Particle Versus Cholesterol Concentration for the Prediction of Cardiovascular Disease in Patients With Metabolic Syndrome and Diabetes Mellitus (from the Multi-Ethnic Study of Atherosclerosis [MESA]). Am J Cardiol (2016) 117(12):1921-7.
12. Urbina EM, McCoy CE, Gao Z et al. Lipoprotein particle number and size predict vascular structure and function better than traditional lipids in adolescents and young adults. J Clin Lipidol (2017) 11(4):1023-1031.
13. Mackey RH, McTigue KM, Chang YF et al. Lipoprotein particles and size, total and high molecular weight adiponectin, and leptin in relation to incident coronary heart disease among severely obese postmenopausal women: The Women's Health Initiative Observational Study. BBA Clin (2015) 3:243-250.
14. Mora S, Caulfield MP, Wohlgemuth J et al. Atherogenic Lipoprotein Subfractions Determined by Ion Mobility and First Cardiovascular Events After Random

Allocation to High-Intensity Statin or Placebo: The Justification for the Use of Statins in Prevention: An Intervention Trial Evaluating Rosuvastatin (JUPITER) Trial. Circulation (2015) 132(23):2220-9.

15. Siurana JM, Ventura PS, Yeste D et al. Myocardial Geometry and Dysfunction in Morbidly Obese Adolescents (BMI 35-40 kg/m^2). Am J Cardiol (2021) 157:128-134.
16. Carrascosa A, Yeste D, Moreno-Galdó A et al. Body mass index and tri-ponderal mass index of 1,453 healthy non-obese, non-undernourished millennial children. The Barcelona longitudinal growth study. An Pediatr (Engl Ed) (2018) 89(3):137-143.
17. Cook S, Weitzman M, Auinger P, Nguyen M, Dietz WH. Prevalence of a metabolic syndrome phenotype in adolescents: findings from the third National Health and Nutrition Examination Survey, 1988-1994. Arch Pediatr Adolesc Med (2003) 157(8):821-7.
18. Lurbe E, Agabiti-Rosei E, Cruickshank JK et al. 2016 European Society of Hypertension guidelines for the management of high blood pressure in children and adolescents. J Hypertens (2016) 34(10):1887-920.
19. Mallol R, Amigó N, Rodríguez MA et al. Liposcale: a novel advanced lipoprotein test based on 2D diffusion-ordered 1H NMR spectroscopy. J Lipid Res (2015) 56(3):737-746.
20. Lorenzo C, Festa A, Hanley AJ, Rewers MJ, Escalante A, Haffner SM. Novel Protein Glycan-Derived Markers of Systemic Inflammation and C-Reactive Protein in Relation to Glycemia, Insulin Resistance, and Insulin Secretion. Diabetes Care (2017) 40(3):375-382.

21. Fuertes-Martín R, Moncayo S, Insenser M et al. Glycoprotein A and B Height-to-Width Ratios as Obesity-Independent Novel Biomarkers of Low-Grade Chronic Inflammation in Women with Polycystic Ovary Syndrome (PCOS). J Proteome Res (2019) 18(11):4038-4045.
22. Amigó N, Fuertes-Martín R, Malo AI et al. Glycoprotein Profile Measured by a 1H-Nuclear Magnetic Resonance Based on Approach in Patients with Diabetes: A New Robust Method to Assess Inflammation. Life (Basel) (2021) 11(12):1407.
23. Malo AI, Girona J, Ibarretxe D et al. Serum glycoproteins A and B assessed by 1H-NMR in familial hypercholesterolemia. Atherosclerosis (2021) 330:1-7.
24. Chamber Quantification Writing Group; American Society of Echocardiography's Guidelines and Standards Committee; European Association of Echocardiography, Lang RM, Bierig M, Devereux RB et al. Recommendations for chamber quantification: a report from the American society of echocardiography's guidelines and standards committee and the chamber quantification writing group, developed in conjunction with the European Association of Echocardiography, a branch of the European Society of Cardiology. J Am Soc Echocardiogr (2005) 18:1440–1463.
25. Khoury PR, Mitsnefes M, Daniels SR, Kimball TR. Age-specific reference intervals for indexed left ventricular mass in children. J Am Soc Echocardiogr (2009) 22:709–714.
26. Daniels SR, Loggie JM, Khoury P, Kimball TR. Left ventricular geometry and severe left ventricular hypertrophy in children and adolescents with essential hypertension. Circulation (1998) 97:1907–1911.

27. Voigt JU, Pedrizzetti G, Lysyansky P et al. Definitions for a common standard for 2D speckle tracking echocardiography: consensus document of the EACVI/ASE/Industry Task Force to standardize deformation imaging. J Am Soc Echocardiogr (2015) 28:183–193.
28. Levy PT, Machefsky A, Sanchez AA et al. Reference Ranges of Left Ventricular Strain Measures by Two-Dimensional Speckle-Tracking Echocardiography in Children: A Systematic Review and Meta-Analysis. J Am Soc Echocardiogr (2016) 29(3):209-225.
29. Shah AS, Davidson WS, Gao Z, Dolan LM, Kimball TR, Urbina EM. Superiority of lipoprotein particle number to detect associations with arterial thickness and stiffness in obese youth with and without prediabetes. J Clin Lipidol (2016) 10(3):610-8.
30. Higgins V, Asgari S, Hamilton JK et al. Postprandial Dyslipidemia, Hyperinsulinemia, and Impaired Gut Peptides/Bile Acids in Adolescents with Obesity. J Clin Endocrinol Metab (2020) 105(4):1228–41.
31. Mietus-Snyder M, Drews KL, Otvos JD et al. Low-density lipoprotein cholesterol versus particle number in middle school children. J Pediatr (2013) 163(2):355-62.
32. Sattar N, Petrie JR, Jaap AJ. The atherogenic lipoprotein phenotype and vascular endothelial dysfunction. Atherosclerosis (1998) 138(2):229-35.
33. Hoogeveen RC, Gaubatz JW, Sun W et al. Small dense low-density lipoprotein-cholesterol concentrations predict risk for coronary heart disease: the Atherosclerosis Risk In Communities (ARIC) study. Arterioscler Thromb Vasc Biol (2014) 34(5):1069-77.

34. Mackey RH, Mora S, Bertoni AG et al. Lipoprotein particles and incident type 2 diabetes in the multi-ethnic study of atherosclerosis. Diabetes Care (2015) 38(4):628-36.

35. Sparks JD, Sparks CE, Adeli K. Selective hepatic insulin resistance, VLDL overproduction, and hypertriglyceridemia. Arterioscler Thromb Vasc Biol (2012) 32(9):2104-12.

36. Rye KA, Barter PJ. Cardioprotective functions of HDLs. J Lipid Res (2014) 55(2):168-79.

37. Rosenson RS, Brewer HB Jr, Ansell B et al. Dysfunctional HDL and atherosclerotic cardiovascular disease. Nat Rev Cardiol (2016) 13(1):48-60.

38. Brown RJ, Rader DJ. When HDL gets fat. Circ Res (2008) 103(2):131-2.

39. Pintó X, Masana L, Civeira F et al. Consensus document of an expert group from the Spanish Society of Arteriosclerosis (SEA) on the clinical use of nuclear magnetic resonance to assess lipoprotein metabolism (Liposcale®). Clin Investig Arterioscler (2020) 32(5):219-229.

40. Amigó N, Mallol R, Heras M et al. Lipoprotein hydrophobic core lipids are partially extruded to surface in smaller HDL: "Herniated" HDL, a common feature in diabetes. Sci Rep (2016) 6:19249.

41. Nobécourt E, Jacqueminet S, Hansel B et al. Defective antioxidative activity of small dense HDL3 particles in type 2 diabetes: relationship to elevated oxidative stress and hyperglycaemia. Diabetologia (2005) 48(3):529-38.

42. Amor AJ, Catalan M, Pérez A et al. Nuclear magnetic resonance lipoprotein abnormalities in newly-diagnosed type 2 diabetes and their association with preclinical carotid atherosclerosis. Atherosclerosis (2016) 247:161-9.

43. Mora S, Glynn RJ, Ridker PM. High-density lipoprotein cholesterol, size, particle number, and residual vascular risk after potent statin therapy. Circulation (2013) 128(11):1189-97.

44. Holmes MV, Millwood IY, Kartsonaki C et al. Lipids, Lipoproteins, and Metabolites and Risk of Myocardial Infarction and Stroke. J Am Coll Cardiol (2018) 71(6):620-632.

45. Davidson WS, Heink A, Sexmith H et al. Obesity is associated with an altered HDL subspecies profile among adolescents with metabolic disease. J Lipid Res (2017) 58(9):1916-1923.

46. Aday AW, Lawler PR, Cook NR, Ridker PM, Mora S, Pradhan AD. Lipoprotein Particle Profiles, Standard Lipids, and Peripheral Artery Disease Incidence. Circulation (2018) 138(21):2330-2341.

47. Varbo A, Benn M, Tybjærg-Hansen A, Jørgensen AB, Frikke-Schmidt R, Nordestgaard BG. Remnant cholesterol as a causal risk factor for ischemic heart disease. J Am Coll Cardiol (2013) 61(4):427-436.

48. Singh GK, Cupps B, Pasque M, Woodard PK, Holland MR, Ludomirsky A. Accuracy and reproducibility of strain by speckle tracking in pediatric subjects with normal heart and single ventricular physiology: a two-dimensional speckle-tracking echocardiography and magnetic resonance imaging correlative study. J Am Soc Echocardiogr (2010) 23(11):1143-52.

49. Puig-Jové C, Castelblanco E, Falguera M et al. Advanced lipoprotein profile in individuals with normal and impaired glucose metabolism. Rev Esp Cardiol (Engl Ed) (2022) 75(1):22-30.

9.3 Myocardial Tissue Characterization and Pericardial Fat Study

1. Maron BJ, Towbin JA, Thiene G et al. Contemporary definitions and classification of the cardiomyopathies: an American Heart Association Scientific Statement from the Council on Clinical Cardiology, Heart Failure and Transplantation Committee; Quality of Care and Outcomes Research and Functional Genomics and Translational Biology Interdisciplinary Working Groups; and Council on Epidemiology and Prevention. Circulation. 2006;113(14):1807-16.
2. Weber KT, Jalil JE, Janicki JS, Pick R. Myocardial collagen remodeling in pressure overload hypertrophy. A case for interstitial heart disease. Am J Hypertens. 1989;2(12 Pt 1):931-40.
3. Taylor AJ, Salerno M, Dharmakumar R, Jerosch-Herold M. T1 Mapping: Basic Techniques and Clinical Applications. JACC Cardiovasc Imaging. 2016;9(1):67-81.
4. Jellis CL, Kwon DH. Myocardial T1 mapping: modalities and clinical applications. Cardiovasc Diagn Ther. 2014;4(2):126–137
5. Aherne E, Chow K, Carr J. Cardiac T1 mapping: Techniques and applications. J Magn Reson Imaging. 2020;51(5):1336-1356.
6. van den Boomen M, Slart RHJA, Hulleman EV et al. Native T1 reference values for nonischemic cardiomyopathies and populations with increased cardiovascular risk: A systematic review and meta-analysis. J Magn Reson Imaging. 2018;47(4):891-912.

7. Puntmann VO, Carr-White G, Jabbour A et al; International T1 Multicentre CMR Outcome Study. T1-Mapping and Outcome in Nonischemic Cardiomyopathy: All-Cause Mortality and Heart Failure. JACC Cardiovasc Imaging. 2016;9(1):40-50.
8. Rodrigues JC, Amadu AM, Ghosh Dastidar A et al. ECG strain pattern in hypertension is associated with myocardial cellular expansion and diffuse interstitial fibrosis: a multi-parametric cardiac magnetic resonance study. Eur Heart J Cardiovasc Imaging. 2017;18(4):441-450.
9. Germain P, El Ghannudi S, Jeung MY et al. Native T1 mapping of the heart - a pictorial review. Clin Med Insights Cardiol. 2014;8(Suppl 4):1-11.
10. Hotamisligil GS. Inflammation, metaflammation and immunometabolic disorders. Nature. 2017 Feb 8;542(7640):177-185.
11. Khan JN, Wilmot EG, Leggate M et al. Subclinical diastolic dysfunction in young adults with Type 2 diabetes mellitus: a multiparametric contrast-enhanced cardiovascular magnetic resonance pilot study assessing potential mechanisms. Eur Heart J Cardiovasc Imaging. 2014;15(11):1263-9.
12. Homsi R, Yuecel S, Schlesinger-Irsch U et al. Epicardial fat, left ventricular strain, and T1-relaxation times in obese individuals with a normal ejection fraction. Acta Radiol. 2019;60(10):1251-1257.
13. Toemen L, Santos S, Roest AAW et al. Pericardial adipose tissue, cardiac structures, and cardiovascular risk factors in school-age children. Eur Heart J Cardiovasc Imaging. 2021;22(3):307-313.
14. Carrascosa A, Yeste D, Moreno-Galdo A et al. Body mass index and tri-ponderal mass index of 1,453 healthy non-obese, non-undernourished millennial children. The Barcelona longitudinal growth study. An Pediatr (Bar) 2018;89:137–143.

15. Siurana JM, Ventura PS, Yeste D et al. Myocardial Geometry and Dysfunction in Morbidly Obese Adolescents (BMI 35-40 kg/m2). Am J Cardiol. 2021;157:128-134.
16. Lurbe E, Agabiti-Rosei E, Cruickshank JK et al. 2016 European Society of Hypertension guidelines for the management of high blood pressure in children and adolescents. J Hypertens. 2016;34(10):1887-920.
17. Mallol R, Amigo N, Rodrıguez MA et al. Liposcale: a novel advanced lipoprotein test based on 2D diffusion-ordered 1H NMR spectroscopy. J Lipid Res. 2015;56:737–746.
18. Gehan EA, George SL. Estimation of human body surface area from height and weight. Cancer Chemother Rep. 1970;54(4):225-35.
19. Dabir D, Child N, Kalra A et al. Reference values for healthy human myocardium using a T1 mapping methodology: results from the International T1 Multicenter cardiovascular magnetic resonance study. J Cardiovasc Magn Reson. 2014;16(1):69.
20. Moon JC, Messroghli DR, Kellman P et al; Society for Cardiovascular Magnetic Resonance Imaging; Cardiovascular Magnetic Resonance Working Group of the European Society of Cardiology. Myocardial T1 mapping and extracellular volume quantification: a Society for Cardiovascular Magnetic Resonance (SCMR) and CMR Working Group of the European Society of Cardiology consensus statement. J Cardiovasc Magn Reson. 2013;15(1):92.
21. Wells JC, Cole TJ; ALSPAC study steam. Adjustment of fat-free mass and fat mass for height in children aged 8 y. Int J Obes Relat Metab Disord. 2002;26(7):947-52.
22. Wu H, Ballantyne CM. Metabolic Inflammation and Insulin Resistance in Obesity. Circ Res. 2020;126(11):1549-1564.

23. Iozzo P. Myocardial, perivascular, and epicardial fat. Diabetes Care. 2011;34 Suppl 2(Suppl 2):S371-9.
24. Baci D, Bosi A, Parisi L, Buono G, Mortara L, Ambrosio G, Bruno A. Innate Immunity Effector Cells as Inflammatory Drivers of Cardiac Fibrosis. Int J Mol Sci. 2020;21(19):7165.
25. Sado DM, White SK, Piechnik SK et al. Identification and assessment of Anderson-Fabry disease by cardiovascular magnetic resonance noncontrast myocardial T1 mapping. Circ Cardiovasc Imaging. 2013;6(3):392-8.
26. Olivotto I, Maron BJ, Tomberli B et al. Obesity and its association to phenotype and clinical course in hypertrophic cardiomyopathy. J Am Coll Cardiol. 2013;62(5):449-57.
27. Parekh K, Markl M, Deng J, de Freitas RA, Rigsby CK. T1 mapping in children and young adults with hypertrophic cardiomyopathy. Int J Cardiovasc Imaging. 2017;33(1):109-117.
28. Cornicelli MD, Rigsby CK, Rychlik K, Pahl E, Robinson JD. Diagnostic performance of cardiovascular magnetic resonance native T1 and T2 mapping in pediatric patients with acute myocarditis. J Cardiovasc Magn Reson. 2019;21(1):40.
29. Levelt E, Mahmod M, Piechnik SK et al. Relationship Between Left Ventricular Structural and Metabolic Remodeling in Type 2 Diabetes. Diabetes. 2016;65(1):44-52.
30. Sunthankar S, Parra DA, George-Durrett K et al. Tissue characterisation and myocardial mechanics using cardiac MRI in children with hypertrophic cardiomyopathy. Cardiol Young. 2019;29(12):1459-1467.

31. Anversa P, Nadal-Ginard B. Myocyte renewal and ventricular remodelling. Nature. 2002 Jan 10;415(6868):240-3.

32. Yeste D, Clemente M, Campos A et al. Diagnostic accuracy of the tri-ponderal mass index in identifying the unhealthy metabolic obese phenotype in obese patients. An Pediatr (Engl Ed). 2021;94(2):68-74.

33. López-Cuenca Á, Manzano-Fernández S, Lip GY et al. Interleukin-6 and high-sensitivity C-reactive protein for the prediction of outcomes in non-ST-segment elevation acute coronary syndromes. Rev Esp Cardiol (Engl Ed). 2013;66(3):185-92.

34. Fox CS, Gona P, Hoffmann U, Porter SA et al. Pericardial fat, intrathoracic fat, and measures of left ventricular structure and function: the Framingham Heart Study. Circulation. 2009;119(12):1586-91.

35. Kleiner DE, Brunt EM, Van Natta M et al; Nonalcoholic Steatohepatitis Clinical Research Network. Design and validation of a histological scoring system for nonalcoholic fatty liver disease. Hepatology. 2005;41(6):1313-21.

36. Ambale Venkatesh B, Volpe GJ, Donekal S et al. Association of longitudinal changes in left ventricular structure and function with myocardial fibrosis: the Multi-Ethnic Study of Atherosclerosis study. Hypertension. 2014;64(3):508-15.

37. Gottbrecht M, Kramer CM, Salerno M. Native T1 and Extracellular Volume Measurements by Cardiac MRI in Healthy Adults: A Meta-Analysis. Radiology. 2019;290(2):317-326.

38. Rosmini S, Bulluck H, Captur G et al. Myocardial native T1 and extracellular volume with healthy ageing and gender. Eur Heart J Cardiovasc Imaging. 2018;19(6):615-621.

39. Tribuna L, Oliveira PB, Iruela A, Marques J, Santos P, Teixeira T. Reference Values of Native T1 at 3T Cardiac Magnetic Resonance-Standardization Considerations between Different Vendors. Diagnostics (Basel). 2021;11(12):2334.
40. Piechnik SK, Ferreira VM, Lewandowski AJ et al. Normal variation of magnetic resonance T1 relaxation times in the human population at 1.5 T using ShMOLLI. J Cardiovasc Magn Reson. 2013;15(1):13.
41. Wells JC. Sexual dimorphism of body composition. Best Pract Res Clin Endocrinol Metab. 2007 Sep;21(3):415-30.